



**TECHNICAL AND VOCATIONAL TRAINING
INSTITUTE (TVTI)**

School of Graduate Studies

**FACULTY OF ELECTRICAL AND ELECTRONICS TECHNOLOGY
AND INFORMATION AND COMMUNICATION TECHNOLOGY
(DEPARTMENT OF ELECTRICAL AND ELECTRONICS
TECHNOLOGY)**

**Voltage Control Of DC-DC Buck Converter Using Super-Twisting Sliding
Mode Control**

MSc Thesis for the Partial Fulfillment of
Master of Science in Electrical Automation and Control Technology
Management

By,

Ali Workineh Beyene (MTR/038/13)

Supervisor,

Chala Merga (Dr.)

AUGUST 2022
Addis Ababa, Ethiopia



**Voltage Control of DC-DC Buck Converter Using Super-twisting Sliding
Mode control**

A Thesis submitted to

**TECHNICAL AND VOCATIONAL TRAINING INSTITUTE (TVTI)
FACULTY OF ELECTRICAL AND ELECTRONICS TECHNOLOGY
AND INFORMATION AND COMMUNICATION TECHNOLOGY
(DEPARTMENT OF ELECTRICAL AND ELECTRONICS
TECHNOLOGY)**

In partial fulfillment for the Degree

**MASTER OF SCIENCE in ELECTRICAL AUTOMATION AND
CONTROL TECHNOLOGY MANAGEMENT**

By,

Ali Workineh Beyene (MRT/038/13)

Supervisor,

Chala Merga (Dr.)

DECLARATION

I hereby declare that the work which is being presented in this thesis entitled ” **Voltage Control of DC-DC Buck Convertor Using Super-twisting Sliding Mode control**” is the original work of my own, has not been presented for a masters thesis in this or other universities and all sources of materials used for this thesis work have been fully acknowledged.

Name: Ali Workineh Beyene (MTR/038/13)

Signature: _____

Place: Addis Ababa

Date of Submission: _____

This thesis proposal has been submitted for examination with my approval as a TVTI advisor.



Chala Merga (Dr.)

Advisor Name

Signature

Date

**TECHNICAL AND VOCATIONAL TRAINING INSTITUTE (TVTI)
FACULTY OF ELECTRICAL AND ELECTRONICS TECHNOLOGY AND
INFORMATION AND COMMUNICATION TECHNOLOGY
(DEPARTMENT OF ELECTRICAL AND ELECTRONICS TECHNOLOGY)**




Thesis on

**Voltage Control of DC-DC Buck Converter Using Super-Twisting Sliding
Mode control**

By,

Ali Workineh Beyene (MTR/038/13)

APPROVED BY THESIS ADVISOR COMMITTEE

Name of the Advisor	Signature	Date
Chala Merga (Dr.)		-----
Name of Examiner Internal		Date
Dr.petchninathan Govindan		-----
Name of Examiner, Internal	Signature	Date
Mr. Tesfaye Nafo	-----	-----
Name of Examiner, External	Signature	Date
Dr. Bisrat Gezahegn		-----
Name of Chairperson	Signature	Date
-----	-----	-----

ACKNOWLEDGEMENT

First and foremost, I would like to express our deep whole hearted gratitude to my advisor Dr.Chala Merga for sharing their unreserved skill, experience and knowledge. His guidance and support was a vital input to perform the work that is without their devoted participation this research may not be implemented.

My appreciation also extends to my parents and relatives who support and encourage me to complete this thesis in particular and the society in general. At last but not least, to start and to complete every activity, it is up on him, since my effort is blessed I am lucky, as a result it becomes tangible now and tomorrow it may be a vital ingredient for further implementation to simplify life, for all thanks God!

ABSTRACT

Non-linear DC-DC converters are employed in any case where it is necessary to stabilize a supplied DC voltage to a specific value. This converter output voltage alone typically oscillates, has significant overshoot, and takes a long time to stabilize. Additionally, when the supply voltage and load vary, it cannot provide the desired output voltage. Numerous controllers are needed to manage this issue and achieve continuous, stable output voltage and quick reaction. Due to their simplicity, FOPID controllers have typically been used with converters to get the desired output voltage. However, the use of FOPID controllers in non-linear systems does not satisfy. In order to improve system efficiency, non-linear controls are necessary. In this study to provide quick and reliable buck converter efficiency, a super-twisting sliding mode controller based on the super-twisting algorithm has been developed. MATLAB/Simulink is used to evaluate the performance of the proposed controller to that of the FOPID controller based on the system's dynamic response in within the overshoot, rising time, settling time, and voltage divergence compare with the setpoint. To test the efficiency of STSM controller increased the load resistance by 30% and reduced by 50% from functional point. Whereas, increased input voltage by 6.28% and decreased by 3.38% from functional point. When the input voltage is 207V, the efficiency of STSM controller the rise (0.0187s) and settling time (0.0229s) are improved compared with FOPID controller. The FOPID controller reduces the overshoot from 140.896 to 15.741 percent, the rising and settling time are 0.1600s and 0.196s respectively and when the input voltage is 220V the overshoot increased from 15.741% to 19.811% using FOPID, whereas the STSM controller completely eliminates the overshoot and chattering effect.

In general based on the results, it can be said that the STSM controller Performance is better than the FOPID controller.

Key words: *Super twisting Sliding Mode control, FOPID controller, DC-DC buck convertor*

TABLE OF CONTENTS

ACKNOWLEDGEMENT	v
ABSTRACT	vi
TABLE OF CONTENTS	vii
List of tables	x
SYMBOL AND ABBREVIATIONS	xi
CHAPTER ONE.....	1
INTRODUCION.....	1
1.1 BACKGROUND	1
1.3 Objective.....	3
1.3.1 General Objective.....	3
1.3.2 Specific Objective.....	3
1.3 Problem of Statement	3
1.4 Significance of the Study.....	3
1.5 Scope of the thesis	3
1.6 Limitation of the thesis	3
1.7 Methodology.....	4
1.8 Outline of theThesis.....	4
CHAPTER TWO	5
LITERATURE REVIEW	5
2.1 SUMMARY OF LITERATURE REVIEW.....	8
CHAPTER THREE	9
MODELING	9
3.1 Buck Converter Mathematical Modeling.....	9
3.1.1 Average Model of Buck Converter.....	13
3.1.2 Procedure for State-Space Averaging.....	14

3.2	Overall System Software Simulation Modeling and Design	17
3.2.1	MATLAB/SIMULINK Model	17
	CONTROLLER DESIGN	18
4.1	Fractional Order PID (FOPID) Controller	18
4.2	Buck Regulator Parameters	21
4.3	Design of STSM Controller for a Buck Convertor	22
4.2.1	The sliding surface's design	22
4.3.2	The control law design.....	23
	CHAPTER FIVE	26
	RESULTS AND DISCUSSION	26
5.1	Buck Converter Open Loop Performance.....	26
5.2	Variation of Load Resistance and Input Voltage in an Open Loop Buck convertor	26
5.3	Buck converter efficiency with a FOPID controller	29
5.4	Buck Converter Performance using FOPID Controller Under Load Resistance and Input Voltage Disturbances.....	31
5.5	Buck Converter Performance using Super -Twisting Sliding Mode Controller	34
5.5	Buck Converter Performance with Super Twisting sliding Mode Controller with Load Resistance and Input Voltage Disturbances.....	35
5.7	Performance analysis of FOPID and STSM Controllers	38
	CHAPTER SIX.....	42
	CONCLUSION AND FUTURE SCOPE	42
6.1	CONCLUSION.....	42
6.2	FUTURE SCOPE	42
	REFERENCE	43
	Appendix	46

List of figures

Figure 1.1: methodology	4
Figure 3.2: off state of buck converter	9
Figure 3.2: On stae of buck converter	10
Figure 3.3: Buck regulator circuit configuration	11
Figure 3.4: Matlab/Simulink Buck DC-Dc Converter Model.....	17
Figure 4.1: control system structure.	18
Figure 4.2: Block diagram of a buck converter.....	22
Figure 5.1: open loop output voltage.	26
Figure 5.3: the input voltage raising from 207 into 220V	27
Figure 5.4: the input voltage drop from 207 into 200V	27
Figure 5.5: Load resistance raised from 10 into 13.....	28
Figure 5.6: Load resistance reduced from 10 into 5.....	28
Figure 5.6: Buck converter model in MATLAB/Simulink with FOPID	29
Figure 5.7: Buck converter output voltage using FOPID	30
Figure .5.8: Buck converter simulation results with FOPID by varing load resistance and input voltage.....	33
Figure 5.9: Buck converter model in MATLAB/Simulink with Super Twisting sliding mode controller	34
Figure 5.10: the buck converter's output voltage using Super Twisting sliding mode controller.	35
Figure 5.11: simulation results of a buck convertor using super-twisting sliding mode controller with varying load resistance and input voltage	37
Figure 5.12: Buck converter output voltage with STSMC & FOPID	40

List of tables

Table 4.1: buck regulator Parameters	21
Table 5.2: FOPID controller parameter	30
Table 5.3: controller performance and output voltage variation.....	38

SYMBOL AND ABBREVIATIONS

ξ	Damping ratio
τ	Sampling time
ΔV	oripple output voltage
ΔQ	change of charge
Δi_L	Peak-to-peak inductor current
V_s	average source voltage
V_{ref}	reference voltage
V_o	actual output voltage
V_L	actual inductor voltage
V_{in}	average input voltage
V_c	average capacitor voltage
V_c	actual capacitor voltage
U	control signal
TSM	Terminal Sliding Mode
T	switching period
STSMC	Super-Twisting Sliding Mode Control
SMPS	Switch mode power supply
SMC	Sliding Mode Control
S	switch
RLS	Recuresive Least Square
R	load resistor
L	Inductor
K_p	Proportional gain
K_i	Integral gain
K_d	Derivative gain
IIR	Infinet Impulse Response
HOSM	Higher Order Sliding Mode
FOPID	Fractional Order Proportional Integral Derivative
FIR	Finit Impulse Response
F	Frequency

DCD	dichotomus coordinate decent
DC	direct current
d	duty cycle
D	average duty cycle
CCM	Continuous Condition Mode
C	Capacitor
t_s	Settling time
t_r	Rise time
t_p	Peak time
L_{min}	Minimum inductor
i_s	Actual input current
I_s	Average input current
I_o	Average output current
i_{Lmin}	Minimum inductor current
i_{Lmax}	Maximum inductor current
i_L	Average inductor current
i_c	Actual Capacitor current
C_{min}	Minimum capacitor

CHAPTER ONE

INTRODUCCION

1.1 BACKGROUND

DC to DC convertor is electronics circuits that change a DC source's voltage from one level into another at the appropriate voltage . Buck conveter is common in power electronics circuits. Due to the fact that all semiconductor components require direct current power, they are now present in practically all electronic devices (DC). Basically, they are applied everywhere a particular DC voltage needs to be stabilized to a specific value. Direct currunt-direct crrent convertor is often utilis in the switch-mode power supplies. In a number of applications, these switch mode direct current-direct current converters are becoming more and more common. Due to the fact that they are used in a variety of applications, including DC motor drives, personal computer power supply, office equipment, appliance control and telecommunications equipment [1][2].

There are numerous types of buck convertor, A three most commonly used ones are the buck, boost, and buck-Boost converters. Buck convertors are a type of chopper circuit that is designed to perform step-down conversion of the applied dc input signal/voltage. There are various power semiconductor devices such as BJT, MOSFET, IGBT and GTO. It serves as a switch in the chopper circuits[3][4].

Fractional order preoportinal integration derivative controller (FOPIDC) helps in achieving the desired results. However it has two drawbacks. The first drawback is that proper control it has high overshoot and it required long time to stable [5]. The high frequency component of the control causes oscillations in the system. Due to this the trajectory of the sliding variable 'S' oscillates in the neighborhood of the desired sliding surface in a zig – zag path instead of remaining on the surface [6]. This phenomenon is known as chattering. Chattering can be reduced by using higher order sliding mode controllers . Using higher order Sliding Mode Control, the continuous approximation of the discontinuous signal is achieved. Various Control Algorithms can be implemented in order to reduce the chattering effect. Some of them are Sub – Optimal algorithm, Twisting algorithm and Super – Twisting algorithm [7]. In case of Sub – Optimal Algorithm, the detection of zeros of 'S' and its derivative is important for the implementation of second order control [7]. The Twisting Algorithm also requires the knowledge of sign of 'S' and its derivative

to define the control law for second order sliding mode control [7]. The Super – Twisting Algorithm requires the relative degree to be equal to one and uses an integration function in the control. The main advantage of this algorithm is that the information of derivative of ‘ S ’ is not mandatory [7].

In this paper, output voltage of DC – DC buck converter is regulated using the Super Twisting Algorithm of Second Order Sliding Mode Control. The effectiveness of the Second Order Sliding Mode Controller as compared with FOPID controllers are demonstrated through simulation results.

1.3 Objective

1.3.1 General Objective

The general objective of the thesis is to develop the buck convertor robustness with input voltage variation and load variation

1.3.2 Specific Objective

This study seeks to develop a system that will address the following:

- To design the mathematical model for buck convertor.
- To develop an output voltage from an open loop buck convertor using MATLAB,
- To design optimization of FOPID controller
- To design a super twisting sliding mode controller for buck convertor voltage regulation.
- To simulate and evaluate the FOPID and STSM controllers using MATLAB.

1.3 Problem of Statement

Power semiconductor components that operate as electronic switches are used to construct DC-DC converters. The buck convertor has an essential nonlinear feature due to the way that switching devices operate. A buck convertor output voltage alone typically oscillates, has a significant overshoot, and takes a long time to stabilize. Additionally, when the input voltage and load change, it cannot deliver the required voltage. As a result, this converter's are needs the controller that have a high level of dynamic response. In order to improve converter performance, a super twisting sliding mode controller for buck converters has been developed in this thesis.

1.4 Significance of the Study

- It ensures that the buck converter output voltage is stable.
- It explains how the buck converter's super twisting sliding mode control law was designed.
- It explains, how get regulated voltage from a buck converter.
- It explains how a buck converter produces controlled voltage.

1.5 Scope of the thesis

To improve the performance of the system controller will be designed using super-twisting sliding mode control. The simulations are going to be carried out by using MATLAB/Simulink software.

1.6 Limitation of the thesis

The system performance results are simulate using software but the results are not implemented in practical.

1.7 Methodology

For the completion of this thesis, the following methodologies were used:

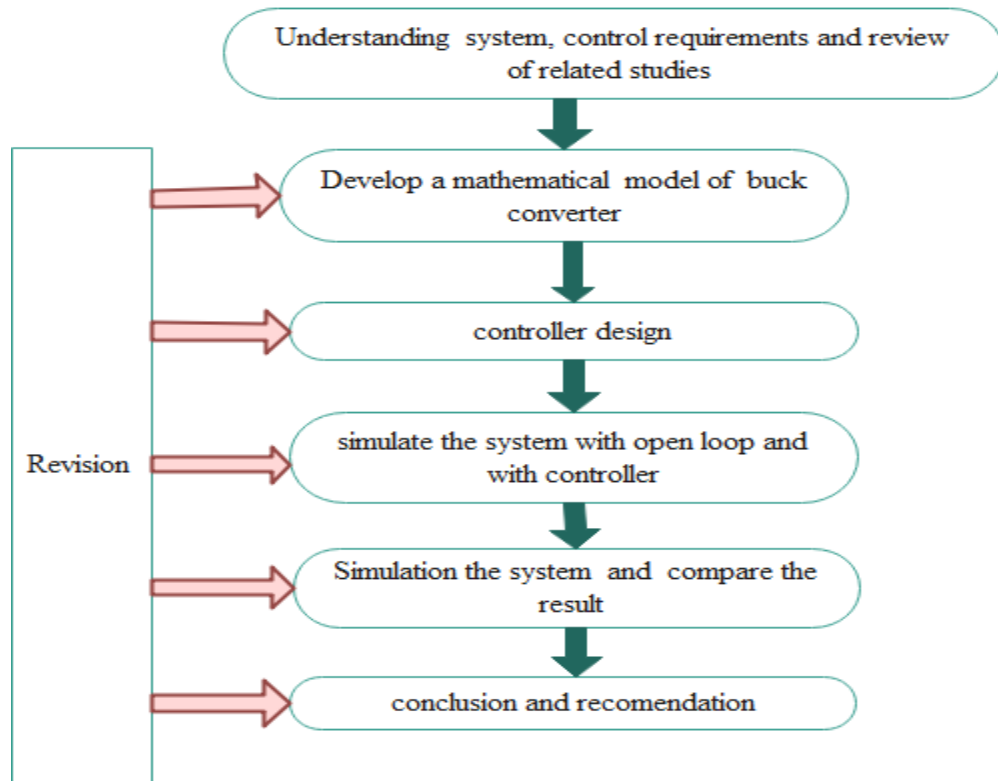


Figure 1.1: methodology

1.8 Outline of the Thesis

This thesis is organized as follows:

Chapter One provides an overview of the study's background. This chapter clearly presents the main parts of the thesis, like the statement of problem, objective, significances of the study, scope and methodology used to complete this study, and study report layout.

Chapter Two includes a review of earlier research and it include the smmery of literature review Chapter Three describes how open loop buck converters, FOPID, and super twisting sliding mode controllers are developed and designed. The proposed controller design is described in Chapter four. the buck converter's outputs with and without FOPID, super-twisting sliding mode controllers been presented in Chapter five. The effectiveness of super-twisting sliding mode controller & FOPID controllers are also evaluated. includes suggestions for additional research at the end. The list of references and supplementary appendices can be found at the conclusion of this thesis report are presented in Chapter Six .

CHAPTER TWO

LITERATURE REVIEW

Researchers have long been interested in the flexibility of DC-DC converter operation and control. Various problems were encountered on the path due to the emerging sophisticated technology in power electronics. In the literature, There are many reducing modeling, develop and control techniques for DC-DC converters. With evolution for microprocessors over the last few decades, much emphasis has been placed on system discretization, This makes controller operating less complicated and faster.

In [8] employs the Buck DC-DC converter using the state-space averaged method to get a state-space averaged small-signal model. To accomplish effective voltage regulation using voltage mode control and he created digital self-tuning PID controllers based on the recursive least squares estimation algorithm. The performance of both self-adapting controllers under varying loads or input voltage was compared in a study. The 1st digitally self-tuning PID controller's improved performance & it has more resistant to model errors also perturbations. In self-tuning and adaptive control methods are more efficient in stable state conditions and the settings are adjusted in accordance with standards, like phase margin and gain margin requirements. As a result, this types of controllers are generally unsuitable for time-varying systems where on-line compensation is desired.

Model reference of adaptive control has received a lot of attention in the field of adaptive control[4]. The main goal of this effort is to minimize and eventually eliminate the difference between the output voltage of the system and the output of the reference model. In this study demonstrates that there is a 0 in the Buck-Boost converter to the right s plane . For evaluating Pole placement controller's unknown parameters using recursive least square method, The author focused on creating an adaptive MRAC controller.

The authors of [8] created a digital control algorithm based on a buck converter's small signal model. In voltage mode control, the preferable output voltage and performance for a buck converter can be expressly specified by the designer controller. In order to reduce the difference between the output voltage and the desired results, this algorithm is used. Additional dynamics can be used to help the controller track load variations and adjust the reference voltage to the changing load, resulting in a zero steady-state error. State feedback is used by the pole placement controller

to choose the weights for the adaptive method. Author [4] focuses on how to design an adaptive control for a buck regulator that is in constant conduction mode. In this study, the author explored the Buck-Boost converter with parasitic and variable load. State space averaging used to convert the system's nonlinear structure into a linear system and identify the regulator parameter quickly. The pole placement controller utilized the control scheme and an recursive least square adaptive filter is used to compute the unknown parameters. According to the author an inventive topology for online system identification.

The author [9] concentrated on computing the dc-dc power converters' parameters using pulse width modulation. The proposed technique has a number of applications, where accurate and precise parameter estimation is required. The suggested method, which is based on the DCD algorithm and uses an Infinite impulse response adaptive filter as the plant model, is computationally effective. Existing RLS algorithms' computational difficulty is reduced by the system identification technique. Importantly, the proposed method can recognize the parameters quickly and precisely.

The author proposed a control technique in that uses pole zero cancellation to cancel the transfer function of the converter. The various methods are discussed in [10], in which a polynomial controller was applied, and its dynamics were contrasted with those of PD & PID controllers. For the voltage-mode switching power supply, a comprehensive state space feedback digital control technique was developed. To cancel out the perturbations and the control design superimposes every switching cycle, a minimal control signal is applied to the control variable's reference value. Furthermore, along with help of extra dynamics, it is possible to guarantee zero steady-state error on the output voltage. The model is defined by a pole assignment on a discrete-time state-variable model. A pole placement control strategy was presented by Kelly and Rinne for to design and operate buck regulator[11]. A feed forward component is used in the control strategy to eliminate the steady state error. The value of the feed forward gain that completely eliminates steady-state error is determined by the plant's gain, which may not be known precisely. The feedforward gain is determined adaptively in this design in order to drive the steady state error to zero. The existing method is simpler than other techniques, and it does not require prior knowledge of system parameters during the adaptation process, however this system have limitations. the controller learns after many repetition and the approach first requires repeatedly perturbing the system [1]. It should have a feed-forward loop included to provide system control & stability

because this design only takes into account PD controllers, which can lead to non-zero steady-state errors. [12] proposed a constant Frequency second-order sliding mode controller for buck regulator using Matlab-Simulink and can reduce the chattering effect of the system but this method causes degradation in the steady-state and transient response. Further to eliminate the chattering effect and to improve the control system performance specification super-twisting sliding mode controller should be designed.

Investigated dual input buck-boost (DIBB) converter using robust chattering free integral sliding mode controller (ISMC) [13]. The simulation results of DIBB for its responses to load and line regulation with improved ISMC are compared with a simulation result of discontinuous control in ISMC. The results show the effectiveness of modified integral sliding mode control with a super-twisting algorithm as a continuous part in ISMC. But the disturbance rejection and tracking performance of the system is not significantly further minimized. [2] employing a terminal sliding mode controller, buck regulator voltage control was examined. A novel twins closed-loop terminal sliding mode (TSM) control method is proposed & compared with the traditional single-loop control method. In this method, the inductance currents & capacitor voltage are the controlled variables for the inner loop subsystem and outer loop subsystem to satisfy the different performance demands, respectively, instead of only choosing one of them, both in the traditional method. Because the inductor and capacitor in a buck convertor are both nonlinear & necessary to be controlled at the same time. Meanwhile, the application of TSM with the advantage of finite-time convergence can improve the response speed & output voltage performance effectively. The simulation result comparisons can confirm the proposed control methods. The steady-state error and rise time can be further improved.

Proposed the development of a fuzzy logic-based sliding mode controller for a DC-DC boost converter. Fuzzy logic aids in lowering the chattering phenomena generated by the sliding mode controller, raising performance and decreasing error, voltage & current ripples [14]. The sliding mode controller ensures robustness against all changes. MATLAB/SIMULINK is used to simulate the suggested system. This model outperforms traditional sliding mode controllers in tests using a range of input and reference voltages. The difficulties may also arise from the lengthy nature of the tuning. Studied saturated dc-dc buck power centers control using PI-type controllers and Σ - Δ Modulation [15]. The controller was developed using two steps that are PI-type controller to regulate the input limited averaged buck convertor system was given and the Σ - Δ modulation was

used to transform the continuous input signal $u_{av}(t)$ into set valued input $u_{sw}(t) \in \{0, 1\}$, which is used to allow the MOSFET gate and its performance result of the system is well. The other reduced the chattering by generating continuous version of the discontinuous control signal in the boundary layer sliding mode controller but this method may cause steady state error [1].

2.1 SUMMARY OF LITERATURE REVIEW

The above-reviewed literature, the voltage control of buck regulator using different controller techniques is discussed. The performances of the system are good enough in terms of transient and steady-state response and they reduced chattering effect when uncertainty happens. In this thesis, super-twisting sliding mode control should be applied to buck converter for voltage control and remove the chattering effect.

CHAPTER THREE

MODELING OF BUCK CONVERTER

this chapter includes, a mathematical model of the buck regulator. Due to their simplicity, FOPID controllers have typically been used with converters to obtain the desired output voltage. However, for non-linear systems the application of FOPID controller is not satisfactory. In order to improve system efficiency, non-linear controls are necessary. To overcome the disadvantages of linear controllers, For buck converters, a nonlinear super twisting sliding mode controller has been developed.

3.1 Buck Converter Mathematical Modeling

DC-DC converters have numerous applications in industry, including electrical machine control, in aviation, as an interface in distributed generation and portable devices. A buck converter (step-down converter) is a dc-to-dc power converter that reduces voltage from input to output. Buck regulators are switched-mode power supply (SMPS) & that contains semiconductor device[16].

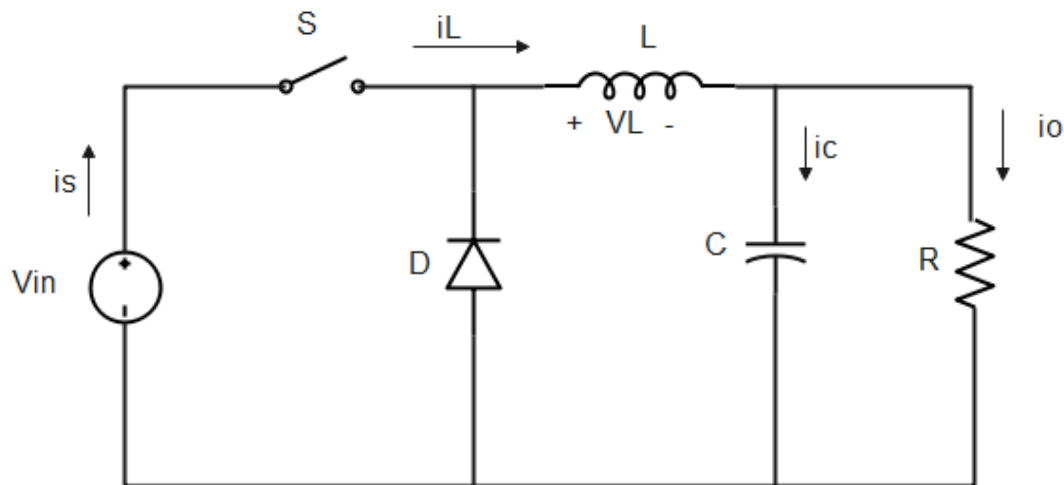


Figure 3.2: off state of buck converter [8][3][6]

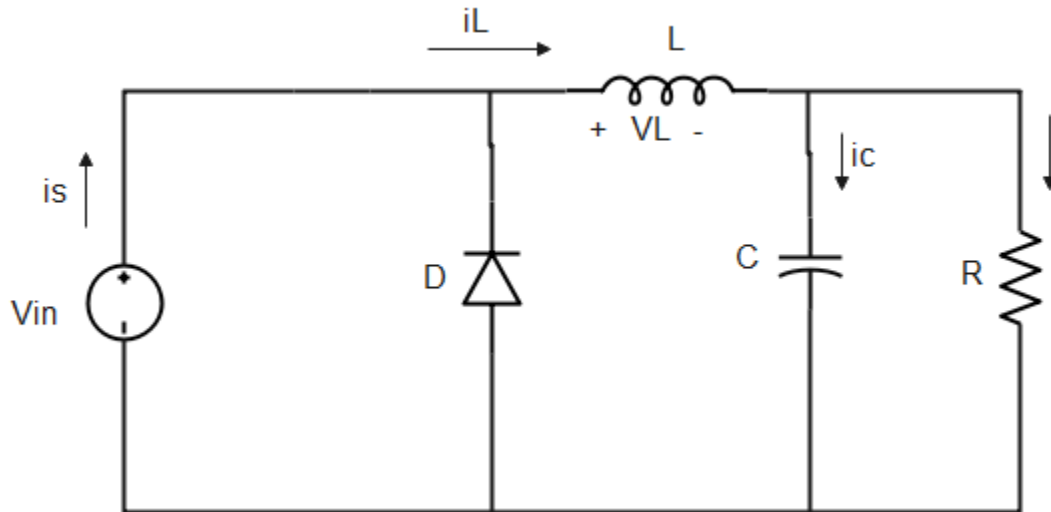


Figure 3.2: On state of buck converter [8][3][6]

The concept of the buck converter is best understood in terms of the current-voltage relationship of the inductor. When the switch is in the off state, the current in the circuit is 0. When the switch is turned on, the current starts to increase, and the inductor responds to the growing current by producing an opposite voltage between its terminals. During this time, the inductor stores energy in the form of a magnetic field. The voltage across the inductor reduces, if the switch is opened while the current is still changing and the net voltage at the load is smaller than the input voltage source. If the switch is in the off position, the voltage across the circuit must be disconnected and the current reduced. A voltage drop through the inductor is caused by the decreasing current. The inductor (opposite to the drop at the on-state) and the inductor is now a source of current. Current flow through the load is supported by the inductor's stored magnetic field energy. When the input voltage source is disconnected, the total current is greater than the average input current (it becomes 0). The "increase" in average current compensates for the voltage drop and ideally maintains the power supplied to the load. The inductor discharges its stored energy into the circuit while it is in the off-state. If the switch is shut off again before the inductor has finished discharging, the voltage at the load is always greater than 0.

figure 3.2 shows the circuit configuration of a buck dc-dc converter.

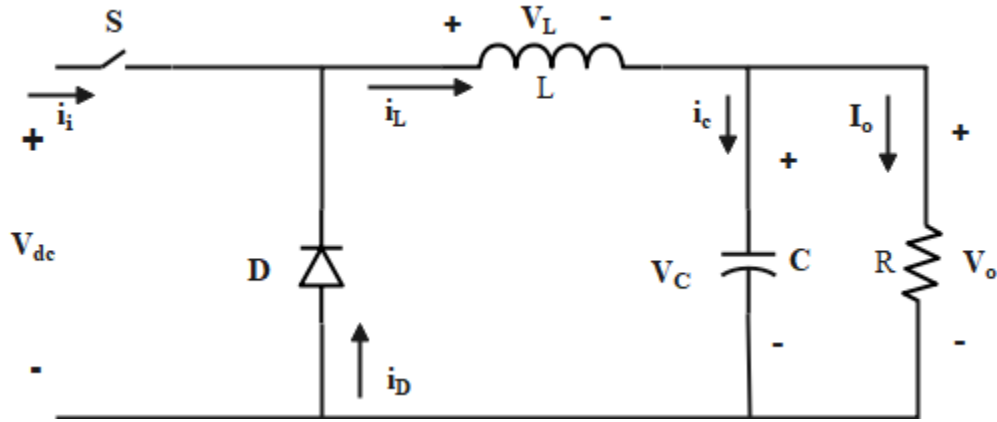


Figure 3.3: Buck regulator circuit configuration[8]

In Figure 3.2 “S” is switch and “D” is diode those are assumed to be ideal & R_L is assumed to be the inductor's equivalent resistance. According to figure 3.2, the kirchhoff's voltage & current laws, difened as:

$$i_L = C \frac{dv}{dt} + \frac{V}{R} \quad (3.1)$$

$$L \frac{di_L}{dt} + R_L i_L + V = f(t) v_d \quad (3.2)$$

The converter switching function $f(t)$ in equation (3.2) defined to determine the convertor relations during on (t_1) & off-state (t_2) switching periods of time , as follows:

$$f(t) = \sum_{n=0}^{\infty} [u(t - nT) - u(t - t_1 - nT)] \quad (3.3)$$

Where n is the number of switching intervals and ‘ T ’ is the switching period. Because the function $f(t)$ has a discontinuous behavior, It exchanges the following variables:

$$t = (n + m)T \quad \text{for } n = 1,1,2 \dots \quad 0 \leq m \leq 1 \quad (3.4)$$

Equation 3.3, $f(t)$ can be rewritten as follows:

$$f(m) \begin{cases} 1 & 0 \leq m \leq D \\ 0 & D \leq m \leq 1 \end{cases} \quad (3.5)$$

D is convertor duty cycle

$$D = \frac{t_1}{T} \quad (3.6)$$

When considering equation 3.5, the interval $[0,1]$ is divided into two intervals $[0, D]$ & $[D, 1]$. The switch “S” will be turned on for the interval $[0, D]$ and turned off for the interval $[D, 1]$. Using

equation 3.4 the value of $f(m)$ in the obtained equations relating to on state and off states of “S”.
The differential equations related to state variables will be given:

$$\begin{aligned} L \frac{di_L(t)}{dt} &= v_m(t) - v_o(t) \\ C \frac{dv_c(t)}{dt} &= i_L(t) - \frac{v_c(t)}{R} \end{aligned} \quad (3.7)$$

Where $V_o(t) = i_o(t)$

state equationis as follow ;

$$\left. \begin{aligned} \frac{di_L(t)}{dt} &= \frac{V_{in}(t)}{L} - \frac{1}{L} V_c(t) \\ \frac{dv_c(t)}{dt} &= \frac{1}{C} i_L(t) - \frac{V_c(t)}{CR} \\ V_o(t) &= V_c(t) \\ i_s(t) &= i_L(t) \end{aligned} \right\} \quad (3.8)$$

Since $V_o(t) = V_c(t)$ state equation matrices will be given as:

$$\left. \begin{aligned} \begin{bmatrix} \frac{dv_o(t)}{dt} \\ \frac{di_L}{dt} \end{bmatrix} &= \begin{bmatrix} -\frac{1}{RC} & \frac{1}{C} \\ -\frac{1}{L} & 0 \end{bmatrix} \begin{bmatrix} V_o(t) \\ i_L(t) \end{bmatrix} + \begin{bmatrix} 0 \\ \frac{1}{L} \end{bmatrix} V_{in}(t) \\ \begin{bmatrix} V_o(t) \\ i_s(t) \end{bmatrix} &= \begin{bmatrix} 0 & 1 \\ 1 & 0 \end{bmatrix} \begin{bmatrix} i_L(t) \\ V_c(t) \end{bmatrix} + \begin{bmatrix} 0 \\ 0 \end{bmatrix} V_{in}(t) \end{aligned} \right\} \quad (3.9)$$

This can be rewritten as;

$$\left. \begin{aligned} \frac{dx(t)}{dt} &= A_1 x(t) + B_1 u(t) \\ y(t) &= C_1 x(t) + D_1 u(t) \end{aligned} \right\} \quad (3.10)$$

Where $A_1 = \begin{bmatrix} -\frac{1}{RC} & \frac{1}{C} \\ -\frac{1}{L} & 0 \end{bmatrix}$, $B_1 = \begin{bmatrix} 0 \\ \frac{1}{L} \end{bmatrix}$, $C_1 = \begin{bmatrix} 0 & 1 \\ 1 & 0 \end{bmatrix}$ and $D_1 = \begin{bmatrix} 0 \\ 0 \end{bmatrix}$

The variable $x(t)$, $u(t)$ and $y(t)$ are the state variables consisting of yield voltages and inductor currents, input voltages to the converers & yield voltages and source currents. Similarly, when the swtich in off position the diode is oprate in forward biased .

the state variables given as:

$$\left. \begin{aligned} L \frac{di_L(t)}{dt} &= -V_c(t) \\ C \frac{dv_c(t)}{dt} &= i_L(t) - \frac{V_c(t)}{R} \\ V_o(t) &= V_c(t) \\ i_s(t) &= 0 \end{aligned} \right\} \quad (3.11)$$

Now substitute $v_o(t)$ instead of $v_c(t)$ the state variables equation given as:

$$\begin{aligned} \begin{bmatrix} \frac{dv_o(t)}{dt} \\ \frac{di_L}{dt} \end{bmatrix} &= \begin{bmatrix} -1 & \frac{1}{C} \\ \frac{RC}{L} & 0 \end{bmatrix} \begin{bmatrix} V_o(t) \\ i_L(t) \end{bmatrix} + \begin{bmatrix} 0 \\ \frac{1}{L} \end{bmatrix} V_{in}(t) \\ \begin{bmatrix} V_o(t) \\ i_s(t) \end{bmatrix} &= \begin{bmatrix} 0 & 1 \\ 0 & 0 \end{bmatrix} \begin{bmatrix} i_L(t) \\ V_C(t) \end{bmatrix} + \begin{bmatrix} 0 \\ 0 \end{bmatrix} V_{in}(t) \end{aligned} \quad (3.12)$$

This can be rewritten as:

$$\left. \begin{aligned} \frac{dx(t)}{dt} &= A_2x(t) + B_2u(t) \\ y(t) &= C_2x(t) + D_2u(t) \end{aligned} \right\} \quad (3.13)$$

Where, $A1 = \begin{bmatrix} -1 & \frac{1}{C} \\ \frac{RC}{L} & 0 \end{bmatrix}$, $B1 = \begin{bmatrix} 0 \\ \frac{1}{L} \end{bmatrix}$, $C1 = \begin{bmatrix} 0 & 1 \\ 0 & 0 \end{bmatrix}$ and $D1 = \begin{bmatrix} 0 \\ 0 \end{bmatrix}$

3.1.1 Average Model of Buck Converter

The weighted average of the two models yields the time averaged system ($S_{average}$), system t_1 and system t_2 with voltage source and without voltage source respectively.

$$S_{avarage} = Dt_1 + (1-D)t_2 \quad (3.14)$$

Using an average state equation over a switching cycle, a state space average model is developed. Use the duty cycle as a weighting factor in state-space averaging, and state equations are combined to create a single averaged state equation. The ABCD matrix of the two systems demonstrates that the B matrices is different, ACD matrices are similar. As a result, the average value of B matrix is all that is required. The following is the state-space averaged equation:

$$B = D.B_1 + (1-D).B_2 \quad (3.15)$$

This can be written as:

$$\left. \begin{aligned} \frac{dx(t)}{dt} &= Ax(t) + Bu(t) \\ y(t) &= Cx(t) + Du(t) \end{aligned} \right\} \quad (3.16)$$

Where; $A = dA_1 + (1-d)A_2$, $B = dB_1 + (1-d)B_2$, $C = dC_1 + (1-d)C_2$ and

$$D = dD_1 + (1-d)D_2$$

$$x(t) = \begin{bmatrix} V_o(t) \\ i_L(t) \end{bmatrix}, \quad u(t) = V_{in}(t), \quad y(t) = \begin{bmatrix} V_o(t) \\ i_s(t) \end{bmatrix} \text{ and } d = \text{duty cycle}$$

Where d is duty cycle

$$\begin{aligned} \begin{bmatrix} \frac{dv_o(t)}{dt} \\ \frac{di_L(t)}{dt} \end{bmatrix} &= \begin{bmatrix} \mathbf{d} \begin{bmatrix} \frac{-1}{RC} & \frac{1}{C} \\ \frac{-1}{L} & \mathbf{0} \end{bmatrix} + (\mathbf{1} - \mathbf{d}) \begin{bmatrix} \frac{-1}{RC} & \frac{1}{C} \\ \frac{-1}{L} & \mathbf{0} \end{bmatrix} \begin{bmatrix} \mathbf{V}_o(t) \\ \mathbf{i}_L(t) \end{bmatrix} + \begin{bmatrix} \mathbf{d} \begin{bmatrix} \mathbf{0} \\ \frac{1}{L} \end{bmatrix} + (\mathbf{1} - \mathbf{d}) \begin{bmatrix} \mathbf{0} \\ \mathbf{0} \end{bmatrix} \mathbf{v}_{in}(t) \begin{bmatrix} \mathbf{V}_o(t) \\ \mathbf{i}_s(t) \end{bmatrix} \\ \begin{bmatrix} \mathbf{d} \begin{bmatrix} \mathbf{0} & \mathbf{1} \\ \mathbf{1} & \mathbf{0} \end{bmatrix} + (\mathbf{1} - \mathbf{d}) \begin{bmatrix} \mathbf{0} & \mathbf{1} \\ \mathbf{0} & \mathbf{0} \end{bmatrix} \begin{bmatrix} \mathbf{i}_L(t) \\ \mathbf{v}_c(t) \end{bmatrix} \end{bmatrix} \end{aligned} \quad (3.17)$$

The state space average model of the convertor is given as :

$$\left. \begin{aligned} \begin{bmatrix} \frac{dv_o(t)}{dt} \\ \frac{di_L(t)}{dt} \end{bmatrix} &= \begin{bmatrix} \frac{1}{RC} & \frac{1}{C} \\ \frac{1}{C} & \mathbf{0} \end{bmatrix} + (1 - D) \begin{bmatrix} \frac{1}{RC} & \frac{1}{C} \\ \frac{1}{C} & \mathbf{0} \end{bmatrix} \begin{bmatrix} v_o(t) \\ i_L(t) \end{bmatrix} + d \begin{bmatrix} \mathbf{0} \\ \frac{1}{L} \end{bmatrix} v_{in}(t) \\ \begin{bmatrix} v_o(t) \\ i_s(t) \end{bmatrix} &= \begin{bmatrix} \mathbf{0} & \mathbf{1} \\ \mathbf{d} & \mathbf{0} \end{bmatrix} \begin{bmatrix} i_L(t) \\ v_c(t) \end{bmatrix} \end{aligned} \right\} \quad (3.18)$$

Then the averaged system given as:

$$\left. \begin{aligned} \frac{dx(t)}{dt} &= Ax(t) + Bu(t) \\ y(t) &= Cx(t) \end{aligned} \right\} \quad (3.19)$$

Because B is the averaged result of the switched system and the input voltage, as well as the capacitor, resistor, and inductor values, So B is determined by duty cycle D, and the value of B changes when duty cycle D changes, making D the control signal. Because the averaged system is a continuous-time system, it must be converted to a discrete-time system.

3.1.2 Procedure for State-Space Averaging

The equivalent state space model is created by averaging the converter's waveform (inductor current and capacitor voltage) over one switching period. As a result, the switching ripples in the waveforms of the voltage and current of the capacitor and inductor will be eliminate[17]. By Using state-space averaging, the power stage which includes the output filter, is linearized. The objective of linearization is to get a small signal transfer function $\frac{\hat{V}_o(s)}{\hat{d}(s)}$.

Where \hat{V}_o & \hat{d} represent small perturbations in the output voltage around their stable state DC operating values V_o & D .

Each circuit (such as RL and Rc) has a state-variable description.

$$\begin{aligned} \dot{x} &= A_1x + B_1x \\ \dot{x} &= A_2x + B_2x \end{aligned}$$

Where, A_1 & A_2 are state matrix ,where B_1 and B_2 are vectors. The output voltage V_o is described as follows;

$$V_o = C_1x$$

$$V_o = c_2 x$$

The duty ratio is used to average the state space equations of both modes. Time weighted averaged equation is;

$$\begin{aligned}\dot{x} &= [A_1 D + A_2(1 - D)]x + [B_1 D + B_2(1 - D)]V_{in} \\ V_o &= [C_1 D + C_2(1 - D)]x\end{aligned}\quad (3.20)$$

The duty ratio “D” used to average the state space equations of both modes. The equation is time weighted and averaged, yielding

$$\begin{aligned}\begin{bmatrix} \frac{d(V_o + \hat{V}_o)}{dt} \\ \frac{d(I_L + \hat{i}_L)}{dt} \end{bmatrix} &= \begin{bmatrix} -1 & 1 \\ \frac{1}{RC} & \frac{1}{C} \\ -1 & 0 \\ L & 0 \end{bmatrix} \begin{bmatrix} V_o + \hat{V}_o \\ I_L + \hat{i}_L \end{bmatrix} + D + \hat{d} \begin{bmatrix} 0 \\ 1 \\ 1 \\ L \end{bmatrix} V_{in} + \hat{V}_{in} \\ \begin{bmatrix} V_o + \hat{V}_o \\ I_S + \hat{i}_s \end{bmatrix} &= \begin{bmatrix} 0 & 1 \\ D + \hat{d} & 0 \end{bmatrix} \begin{bmatrix} I_L + \hat{i}_L \\ V_c + \hat{V}_c \end{bmatrix}\end{aligned}\quad (3.21)$$

Equation 3.21 can be described

$$\begin{aligned}\frac{d(V_o + \hat{V}_o)}{dt} &= -\frac{1}{RC}(V_o + \hat{V}_o) - \frac{1}{L}(I_L + \hat{i}_L) \\ \frac{d(I_L + \hat{i}_L)}{dt} &= -\frac{1}{L}(V_o + \hat{V}_o) + (D + \hat{d})\left(\frac{1}{L}\right)(V_{in} + \hat{V}_{in}) \\ V_o + \hat{V}_o &= V_c + \hat{V}_c \\ I_L + \hat{i}_L &= (D + \hat{d})(I_L + \hat{i}_L)\end{aligned}\quad (3.22)$$

In general, $V_{in} = v_{in} + \hat{v}_{in}$ however, The instability in the input voltage is taken to be zero to determine the transfer function among the voltage V_o and the control input d .

$$\begin{aligned}C \frac{d\hat{V}_o}{dt} &= -\frac{1}{R}(\hat{V}_o) + \hat{i}_L \\ L \frac{d\hat{i}_L}{dt} &= -\hat{V}_o + (D\hat{V}_{in} + \hat{d}V_{in}) \\ \hat{V}_o &= \hat{V}_c \\ \hat{i}_L &= D\hat{i}_L + I_L \hat{d}\end{aligned}\quad (3.23)$$

The Laplace transform Equation 3.23 given as:

$$\begin{aligned}Cs\hat{V}_o(s) &= -\frac{1}{R}\hat{V}_o(s) + \hat{i}_L(s) \\ Cs\hat{i}_L(s) &= -\hat{V}_o(s) + D\hat{V}_{in}(s) + \hat{d}V_{in}(s) \\ \hat{V}_o(s) &= \hat{V}_c(s) \\ \hat{i}_L(s) &= D\hat{i}_L(s) + \hat{d}I_L(s)\end{aligned}\quad (3.24)$$

$$Cs\hat{V}_o(s) = -\frac{1}{R}\hat{V}_o(s) + \hat{i}_L(s) \quad (3.25)$$

$$Ls\hat{i}_L(s) = -\hat{v}_o(s) + D\hat{V}_{in}(s) + \hat{d}V_{in}(s) \quad (3.26)$$

Where, $\hat{d}(s) = 0$ So that so, $Ls\hat{i}_L(s) = -\hat{V}_o(s) + D\hat{V}_{in}(s)$

$$Ls\hat{i}_L(s) = -\hat{V}_o(s) + D\hat{V}_{in}(s)$$

$$\hat{i}_L(s) = D\hat{i}_L(s) + \hat{d} I_L(s)$$

$$\hat{i}_L(s) = D\hat{i}_L(s) \quad (3.27)$$

Equation 3.25 solve for $\hat{i}_L(s)$ gives,

$$Cs\hat{V}_o(s) = -\frac{1}{R}\hat{V}_o(s) + \hat{i}_L(s)$$

$$\hat{i}_L(s) = Cs\hat{V}_o(s) + \frac{1}{R}\hat{V}_o(s)$$

$$\hat{i}_L(s) = \hat{V}_o(s) \left(Cs + \frac{1}{R} \right) \quad (3.28)$$

Substitute for $\hat{i}_L(s)$ into Equation 3.26 from Equation 3.28 gives,

$$Ls\hat{i}_L(s) = -\hat{V}_o(s) + D\hat{V}_{in}(s)$$

$$Ls \left(Cs + \frac{1}{R} \right) \hat{V}_o(s) = -\hat{V}_o(s) + D\hat{V}_{in}(s) \quad (3.29)$$

Once the buck converter's average state space model is defined and the Laplace transform can be used to obtain the frequency response linear time models and the models are critical to design linear feedback control. Locating the poles and zeros for perfect voltage regulation involves using the converters' control to output voltage transfer function[18]. The small signal average model of Buck regulator should be used to determine the control output transfer function using the Laplace transform.

$$\frac{\hat{v}_o(s)}{\hat{v}_m(s)} = D \left[\frac{\frac{1}{LC}}{s^2 + \frac{1}{RC}S + \frac{1}{LC}} \right] \quad (3.30)$$

3.2 Overall System Software Simulation Modeling and Design

3.2.1 MATLAB/SIMULINK Model

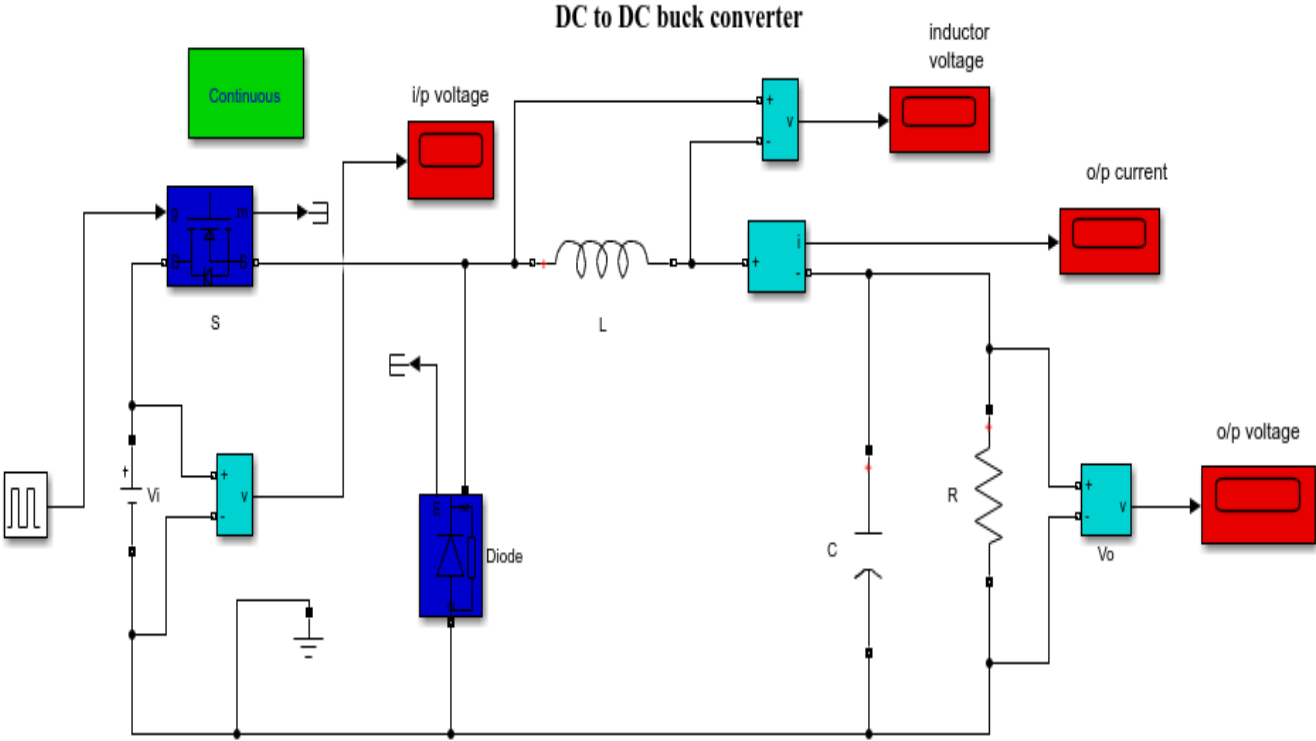


Figure 3.4: Matlab/Simulink Buck DC-Dc Converter Model

CHAPTER FOUR

CONTROLLER DESIGN

4.1 Fractional Order PID (FOPID) Controller

FOPID have five parameters to choose from increases design flexibility and allows the designer to better shape an open-loop transfer function for a specific control task. Tuning the FOPID controllers in terms of design and stability analysis, on the other hand, is more difficult. To address this issue, various design approaches are presented in the literature[5]. This controller includes a transfer function.

$$G_{FOPID}(s) = K_p + \frac{K_i}{s^\lambda} + K_d \times s^\mu \quad (4.1)$$

The value of power in a fractional order controller ranges between [0, 1]. Fractional order PID has five parameters the two additional tuning parameters (μ and λ) that can be used to adjust the control action. The controller's two tuning parameters provide improved control for dynamic systems. As a result, it is a viable alternative to traditional controllers. The basic controller equation is given (4.1).

$$G(s) = \frac{V_{in}}{(as^2+bs+c)} \quad (4.2)$$

Where the coefficient a, b, c given as:

$$a = LC; \quad b = \frac{L}{R} + R_L C; \quad c = 1 + \frac{R_L}{R}$$

The control system structure is shown below in figure 4.1

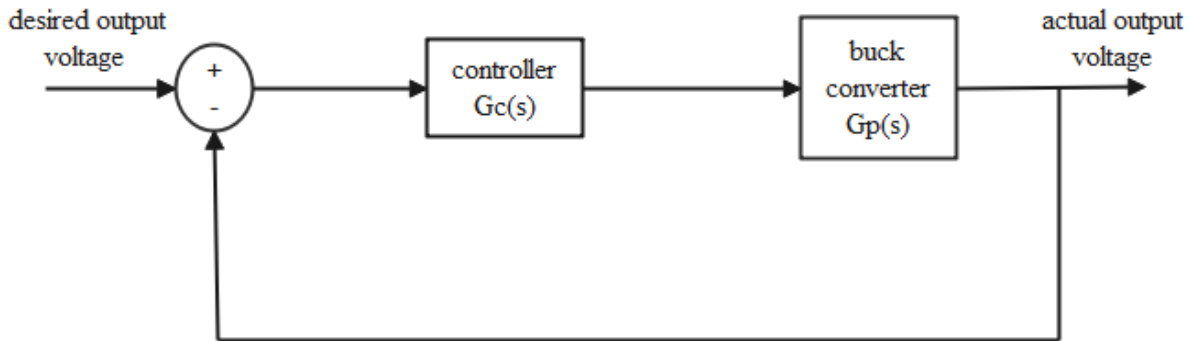


Figure 4.1: control system structure.

The open loop transfer function of buck regulator is stated as;

$$G_p(s) = \frac{\hat{v}_o(s)}{\hat{v}_{in}(s)} = D \left[\frac{\frac{1}{LC}}{s^2 + \frac{1}{RC}s + \frac{1}{LC}} \right] \quad (4.10)$$

The transfer function of FOPID controller need to control plant (G_p). The basic controller equation representation for the respective controllers is given in equation (4.11).

$$G_c(s) = k_p + \frac{k_i}{s^\lambda} + k_d \times s^\mu \quad (\lambda, \mu > 0) \quad (4.11)$$

Where,

k_p : Proportional gain of the FOPID controller

k_i : Integral gain of the FOPID controller

k_d : Derivative gain of the FOPID controller

λ : the order of integral

μ : the order of differentiation.

Equation (4.12) below gives the transfer function for the buck converter.

$$G_p(s) = D \left[\frac{\frac{1}{LC}}{s^2 + \frac{1}{RC}s + \frac{1}{LC}} \right] \quad (4.12)$$

Equation (4.13) below provides the converter's close loop transfer function.

$$G_{cl}(s) = \frac{V(s)}{V_{ref}(s)} = \frac{D \left[\frac{\frac{1}{LC}}{s^2 + \frac{1}{RC}s + \frac{1}{LC}} \right] G_c(s)}{1 + \left[\frac{\frac{1}{LC}}{s^2 + \frac{1}{RC}s + \frac{1}{LC}} \right] G_c(s)}$$

In general second order plant is characterized by the open loop transfer function,

$$G_p(s) = \frac{K}{s^2 + 2\xi^{01}\omega_n^{01}s + (\omega_n^{01})^2} \quad (4.13)$$

Where,

ξ^{01} : Damping ratio of the second order (open loop) plant

ω_n^{01} : Natural frequency of the second order (open loop) plant

K: Gain of the second order (open loop) plant

Then the close loop transfer function becomes

$$G_{cl}(s) = \frac{G_p(s)G_c(s)}{1+G_p(s)G_c(s)} \quad (4.14)$$

Substituting for from Equation (4.11) and (4.13) respectively into Equation (4.14) gives,

$$G_{cl}(s) = \frac{K(K_d s^{\lambda+\mu} + K_p s^\lambda + K_i)}{(s^{4+\lambda} + (2\xi^{01}\omega_n^{01} + KK_d)s^{2+\lambda} + ((\omega_n^{01})^2 + KK_p)s^\lambda + KK_i)} \quad (4.15)$$

From (4.13) it is clear that the open loop plant has two poles at $[-\xi^{01}\omega_n^{01} \pm j\omega_n^{01}\sqrt{1-(\xi^{01})^2}]$ and from (4.11) is also evident that the FOPID controller has one pole at origin and also two zeros $\left[-\frac{K_p}{2K_d} \pm j\sqrt{\frac{K_i}{K_d} - \frac{K_p^2}{4K_d^2}}\right]$. It is considered that both the plant poles and controller zeros are complex conjugates in the complex s-plane. From (4.15), it is seen that the closed loop system has two zeros and three poles in the complex s-plane and position of the closed loop zeros remains unchanged as in (4.11) while position of the closed loop poles changes depending on the FOPID controller gains.

For guaranteed pole placement with PID controllers, the closed loop system (3.26) should have one real pole which should be far away from the real part of the other two complex (conjugate) closed loop poles as discussed in Wang et al. [22]. It is also reported in [22] that the contribution of the real pole in the closed loop dynamics becomes insignificant if magnitude of the real closed loop pole be at least 3-5 (let us call this factor as m „relative dominance“) times greater than real part of the complex closed loop poles.

Now, if the desired closed loop performance of a second order system be given as the specifications on ξ^{cl} (Damping ratio of the closed loop system) and ω_n^{cl} (Natural frequency of the closed loop system) as in [23] one can easily replace the position of the real zero (α) by $(-m\xi^{cl}\omega_n^{cl})$, provided that $\alpha = -m\xi^{cl}\omega_n^{cl}$ is chosen to be large enough with respect to $(\xi^{cl}\omega_n^{cl})$. Therefore, With a proper choice of relative dominance (m), the third order closed loop system (4.15) will behave like an almost second order system having the user specified closed loop damping ratio ξ^{cl} (percentage of maximum overshoot) and closed loop natural frequency ω_n^{cl} (rise time)

$$\left. \begin{aligned} K_p &= \frac{(\omega_n^{cl})^3 + 2m(\xi^{cl})^2(\omega_n^{cl})^4 - (\omega_n^{01})^2}{K} \\ K_i &= \frac{m\xi^{cl}(\omega_n^{cl})^4}{K} \\ K_d &= \frac{(2+m)\xi^{cl}(\omega_n^{cl})^4 - 2\xi^{01}\omega_n^{01}}{K} \end{aligned} \right\} \quad (4.16)$$

4.2 Buck Regulator Parameters

In the table below, the buck converter's selected parameters are listed.

Table 4.1: buck regulator Parameters

Number	Description	parameters	Amount	Unit
1	Input voltage	V_{in}	207	Volts
2	Reference voltage	V_{ref}	103.5	Volts
3	Capacitance	C	250	microfarad
4	Inductance	L	1.5	mH
5	Resistance	R	10	Ohm
6	Frequency	F	100000	HZ
7	Duty Cycle	D	0.5	-

Since the open loop transfer function of buck converter system is given above by Equation (4.12), so Equating it with Equation (4.13) the unknown open loop system parameters k , ξ^{ol} and ω_n^{ol} are obtained. Using the parameters given in table above,

$$K = \frac{D}{LC} = \frac{0.5}{1.5 \times 10^{-3} \times 250 \times 10^{-6}} = 1.33 \times 10^6$$

$$\omega_n^{ol} = \sqrt{\frac{1}{LC}} = \sqrt{\frac{1 \times 10^9}{1.5 \times 250}} = 1.633 \times 10^3$$

$$\xi^{ol} = \frac{1}{2RC\omega_n^{ol}} = \frac{1 \times 10^9}{2 \times 10 \times 250 \times 1.633 \times 10^3} = 0.123$$

Thus, buck convertor transfer function (open loop) is;

$$\mathbf{G_p(s)} = D \left[\frac{\frac{1}{LC}}{s^2 + \frac{1}{RC}S + \frac{1}{LC}} \right]$$

$$\mathbf{G_p(s)} = \frac{1.33 \times 10^6}{s^2 + 400 \times s + 2.667 \times 10^6}$$

Then selecting the desired parameters of closed loop system and using the relations in Equation (4.16) the gains of the PID controller are calculated which produces exact pole placement at desired damping and frequency provided m is chosen iteratively by checking the accuracy of system response. Here the desired parameters of closed loop system chosen are $\xi^{cl} = 0.148$ and $\omega_n^{cl} = 120 \text{ rad/sec}$ selecting appropriate value of the relative dominance by trial and

error by checking the accuracy of system response. For a FOPID controller the integral (λ) and differential (μ) order value varies in between 0 and 1 [5].

The closed loop transfer function becomes described in equation 4.13 will be:

$$G_{cl}(s) = \frac{454.72615s^{0.73284} + 373.4745s^{0.22307} + 472.2615}{1.5 \times 10^{-8} * s^{2.2307} + 1.5 \times 10^{-3} * s^{1.50977} + 10 * s^{0.22307} + 454.72615s^{0.73284} + 373.4745s^{0.22307} + 472.2615} \quad (4.17)$$

4.3 Design of super-twisting sliding mode Controller for a Buck Converter

According to Section (3.3), the buck converter's state space average is as follows:

$$\begin{bmatrix} \dot{x}_1 \\ \dot{x}_2 \end{bmatrix} = \begin{bmatrix} -\frac{1}{RC} & \frac{1}{C} \\ -\frac{1}{L} & 0 \end{bmatrix} \begin{bmatrix} x_1 \\ x_2 \end{bmatrix} + \begin{bmatrix} 0 \\ \frac{d}{L} \end{bmatrix} u \quad (4.18)$$

Where, $[x_1 \ x_2] = [V_o \ i_L]$ and the system's input controls is $u = V_{in}$. A sliding surface is used by the controller in sliding mode control to choose the input states, u to the system. To control “buck converter” efficiently using advanced nonlinear control methods, the mathematical converter model must first be built using the state space equation. As a result, before designing the control law, the sliding surface for the system is created.

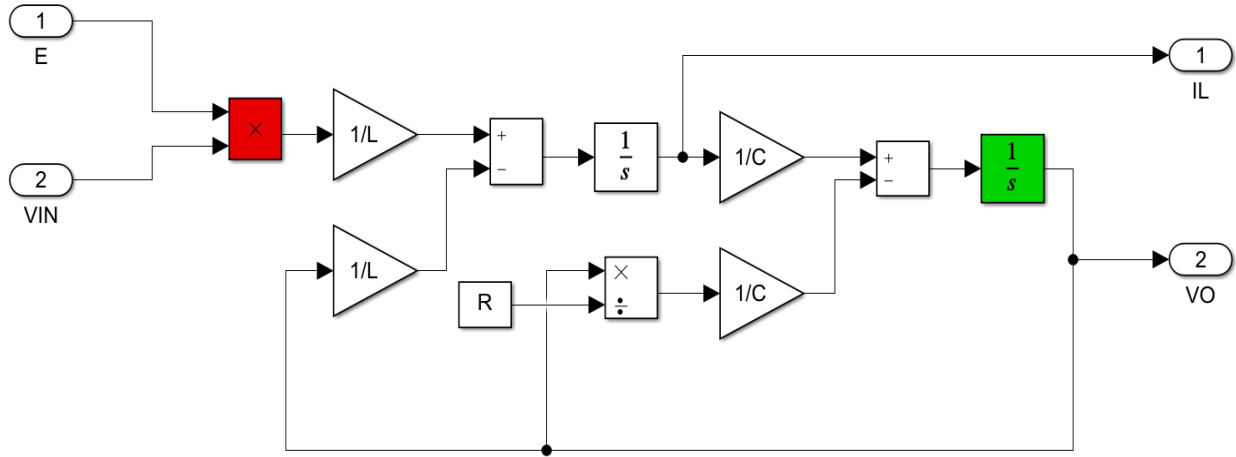


Figure 4.2: Block diagram of a buck converter

4.2.1 The sliding surface's design

The DC-DC buck converter's selected sliding surface for voltage regulation is given:

$$s = X_1 - X_{ref} \quad (4.19)$$

Where, X_1 is output voltage (V_o) and X_{ref} reference voltage/desired output voltage.

The sliding surface's derivative gives as;

$$\dot{s} = \dot{X}_1 - \dot{X}_{ref} \quad (4.20)$$

Since X_{ref} is constant and its derivative $\dot{X}_{ref} = 0$ and replacing with from Equation (4.15) into Equation (4.20) gives,

$$\dot{s} = \frac{-1}{RC}X_1 + \frac{1}{C}X_2 \quad (4.21)$$

The sliding surface's second derivative results is,

$$\ddot{s} = \frac{-1}{RC}x_1 + \frac{1}{C}x_2 \quad (4.22)$$

Insert Equation (4.17) into Equation (4.18) gives,

$$\ddot{s} = \left(\frac{1}{R^2} + \frac{1}{LC} \right) X_1 + \frac{1}{RC^2} X_2 + \frac{d}{LC} u \quad (4.23)$$

$$\ddot{s} = f + gu \quad (4.24)$$

Where,

$$f = \left(\frac{1}{R^2} + \frac{1}{LC} \right) X_1 + \frac{1}{RC^2} X_2 \text{ and}$$

$$g = \frac{d}{LC}$$

Since the system's relative degree is two, a second order sliding mode controller is more appropriate to improving control precision.

4.3.2 The control law design

A modified second order sliding mode control is a super twisting sliding mode control. The sliding mode controller based on the super-twisting algorithm does not require any knowledge of the sliding variable's derivatives[11]. This algorithm's control law consists of 2 terms .that are "ua" defined as a discontinuous time derivative and "ub" defined as a continuous function of sliding variable.

$$u = u_a + u_b \quad (4.25)$$

$$\dot{u}_a = \begin{cases} -u & \text{when } |u| > 1 \\ -K\text{sign}(s) & \text{when } |u| \leq 1 \end{cases} \quad (4.26)$$

$$u_b = \begin{cases} -\lambda|s_o|^\xi \text{sign}(s) & \text{when } |s| > s_o \\ -\lambda|s_o|^\xi \text{sign}(s) & \text{when } |s| \leq s_o \end{cases} \quad (4.27)$$

When $\xi=1$ then this algorithm converges to the origin exponentially and equivalent conditions is;

$$K = \frac{\Phi}{\Gamma_m}, \quad \lambda^2 \geq \frac{4\Phi}{\Gamma_m^2} \frac{\Gamma_m(k + \Phi)}{\Gamma_m(k - \Phi)} \quad 0 < \xi \leq 0.5 \quad (4.28)$$

Where K, λ, s_o, Φ, m are positive constants.

When controlled system was linearly dependent on u , the control law could be simplified[19],[11] as,

$$u = -\lambda|s|^\xi \text{sign}(s) + u_a \quad (4.29)$$

$$\dot{u}_a = -K \text{sign}(s) \quad (4.30)$$

The goal of the control is to achieve the desired output voltage (V_{ref}). At steady state, it described as;

$$E = V_{ref} \quad (4.31)$$

$$\dot{E} = \dot{V}_{rfe} \quad (4.32)$$

Combining equations (4.31) and (3.7) yields the desired output current as

$$i_L^* = \frac{V_{ref}}{R} \quad (4.33)$$

The actual current i_L exactly match the desired current I_L . Sliding mode is an ideal approach for this task, because its exact tracking property. The sliding function can be built using the state variables. The sliding surface for sliding mode current control is selected to be:

$$s = i_L - i_L^* = 0 \quad (4.34)$$

The control signal is used to enforce sliding mode in the manifold the value $s = 0$.

$$u = \frac{1}{2}(1 - \text{sgn}(S)) \quad (4.35)$$

The switching actions is :

$$u = \begin{cases} 0, & s > 0 \\ 1, & s < 0 \end{cases} \quad (4.36)$$

The Lyapunov stability condition, $ss' < 0$, must be satisfied for the phase trajectory to reach the sliding surface. As a result of this,

$$0 < V_0 < E \quad (4.37)$$

This is the sliding mode control's existence condition. V_o must be positive in order for the inequality to hold (4.37). The sliding manifold's attraction domain is defined by (4.35). Because there is no gain in the controller in equation (4.30), the system model determines the domain of attraction. In steady state, the output voltage of buck convertor is smaller than input voltage .

Buck convertor is made up of power switch semiconductor devices that function as electronic switches. As a result, the control signals of the power switch are 1 and 0. If the control signal value is 0, the control switch is at off position and it is 1, the control switch is at on position. A main issue that prevents the widespread use of conventional sliding mode controllers is the high chattering effect, which leads to reduced control accuracy and high switching losses in power circuits. The approach of higher order sliding mode control is one solution to this problem. It retains the same properties as a typical sliding mode controller while also eliminating chattering issues. The second time derivative of the sliding variable is used by the second order sliding mode controller. However, the sliding variable's first time derivatives are also required.

This makes implementing a higher order sliding mode controller a little more complex. A modified second order sliding mode control is a super twisting sliding mode control. The sliding mode controller based on the super-twisting algorithm does not require any knowledge of the sliding variable's derivatives[20]. The control law given in equation (4.34) replaces the controller in equation (4.35). The control law for SMC based on the super twisting algorithm is given by

$$u = -\lambda_1 |s|^{\frac{1}{2}} \text{sgn}(s) + u_a \quad (4.38)$$

$$\dot{u}_a = -\lambda_2 \text{sgn}(s) \quad (4.39)$$

Where λ_1 and λ_2 denote gain constants that are given by

$$\lambda_1 = 1.5\sqrt{L} \quad \lambda_2 = 1.1L \quad \text{or} \quad \lambda_1 = \sqrt{L} \quad \lambda_2 = 2L$$

are valid, L is known as Lipschitz constant, $L > 0$ It can be calculated using the detailed procedure described in [21].

CHAPTER FIVE

RESULTS AND DISCUSSION

5.1 Buck Converter Open Loop Performance

The buck regulator performance in open-loop is examined utilising the MATLAB/Simulink.

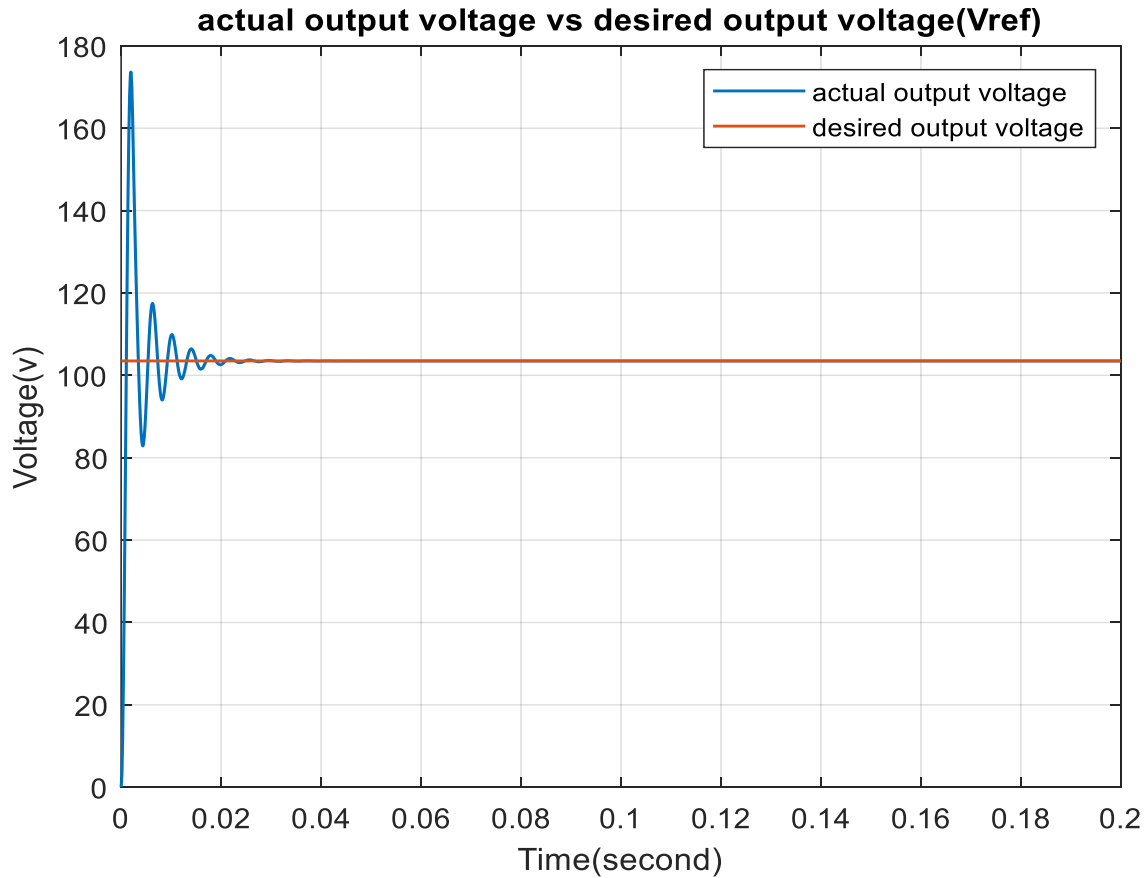


Figure 5.1: open loop output voltage.

Figure 5.1 depicts the result of output voltage with out controller .The output voltage overshoot is 140.896%, and the rise time is 359.966 ms. The time it takes to settle is 17.524 ms. the significant overshoot is not necessary in the output voltage

5.2 Variation of Load Resistance and Input Voltage in an Open Loop Buck convertor

For evaluating the performance of the open-loop buck regulator by changing the input voltage, raising the voltage from 207 into 220V & dropped to 200V and The load resistance is raised from

10 to 13 and then lowered to 5, to testing the impact of load resistance change. Shown in the below figures simulation results.

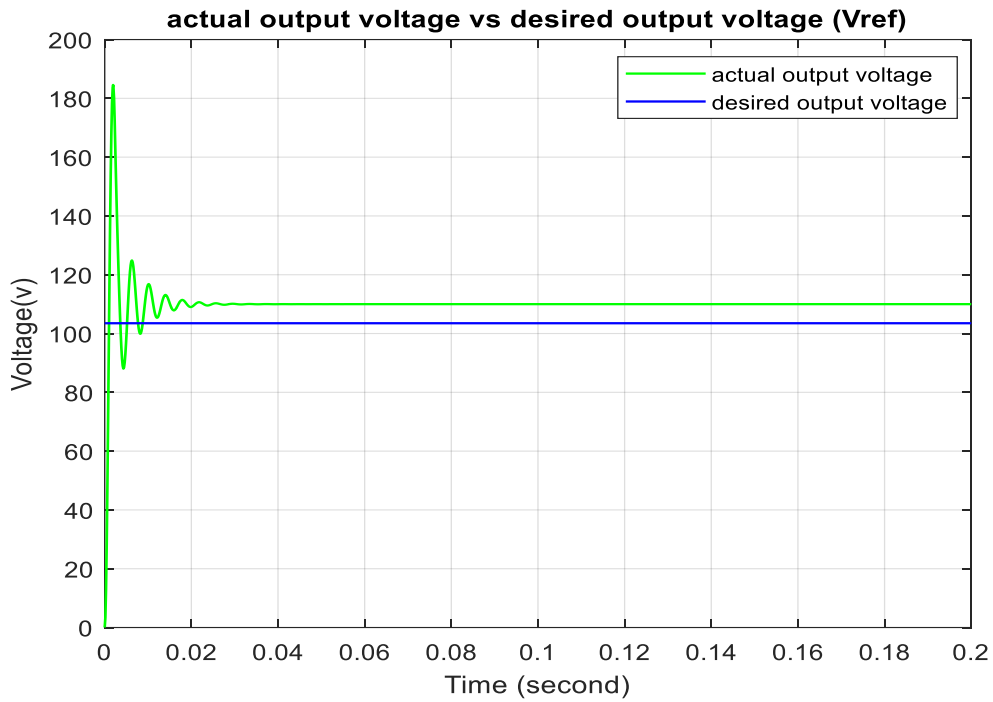


Figure 5.3: the input voltage raising from 207 into 220V

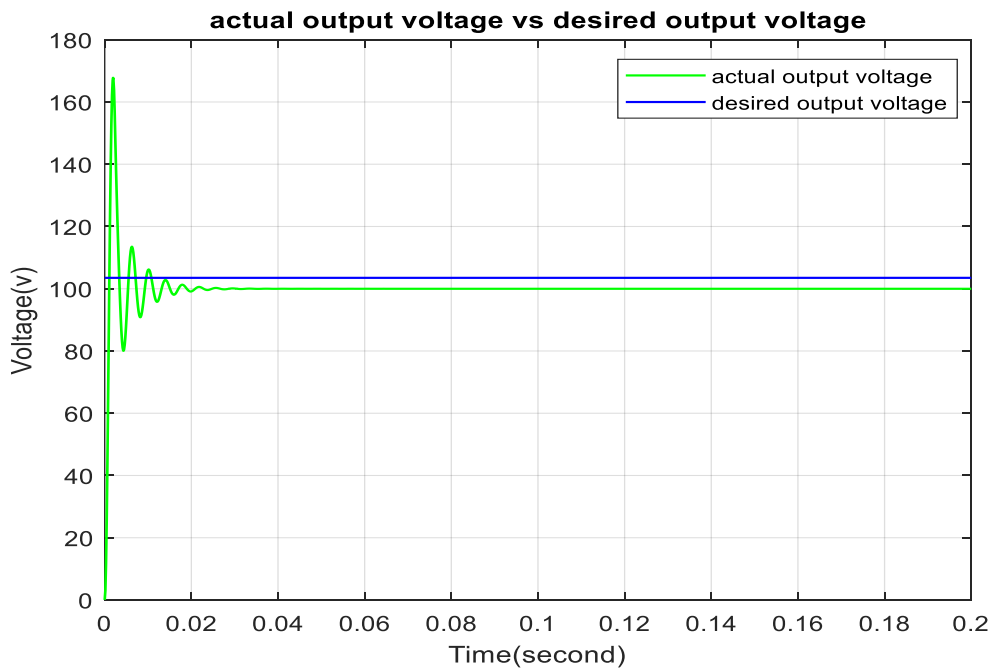


Figure 5.4: the input voltage drop from 207 into 200V

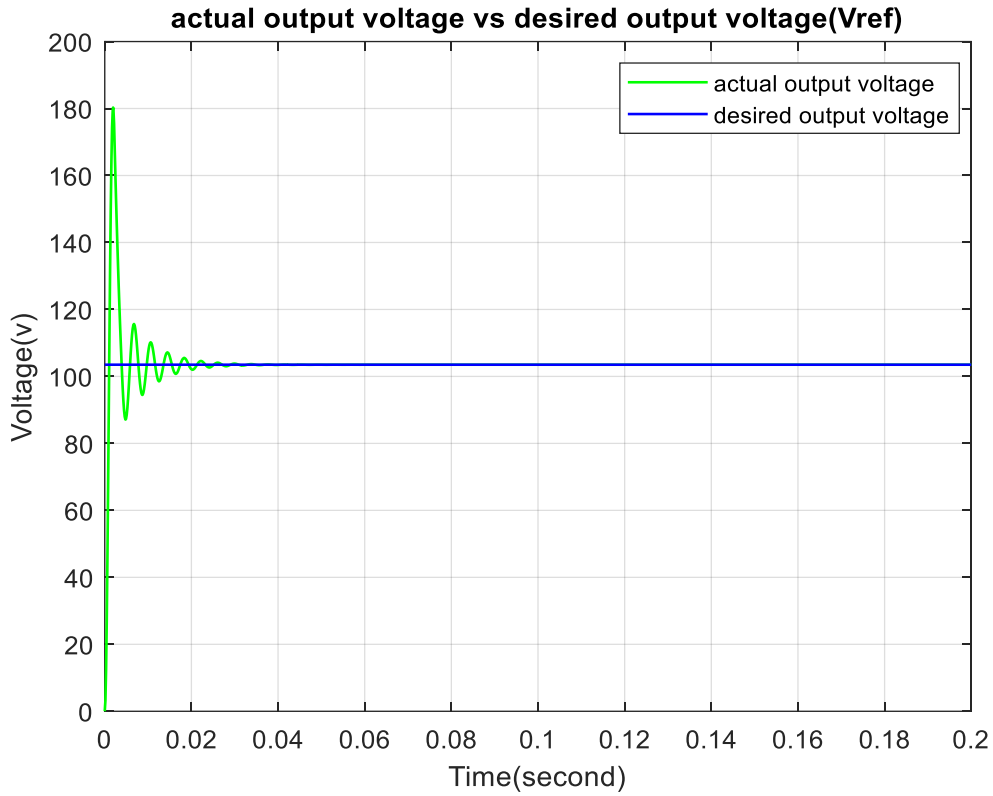


Figure 5.5: Load resistance raised from 10 into 13

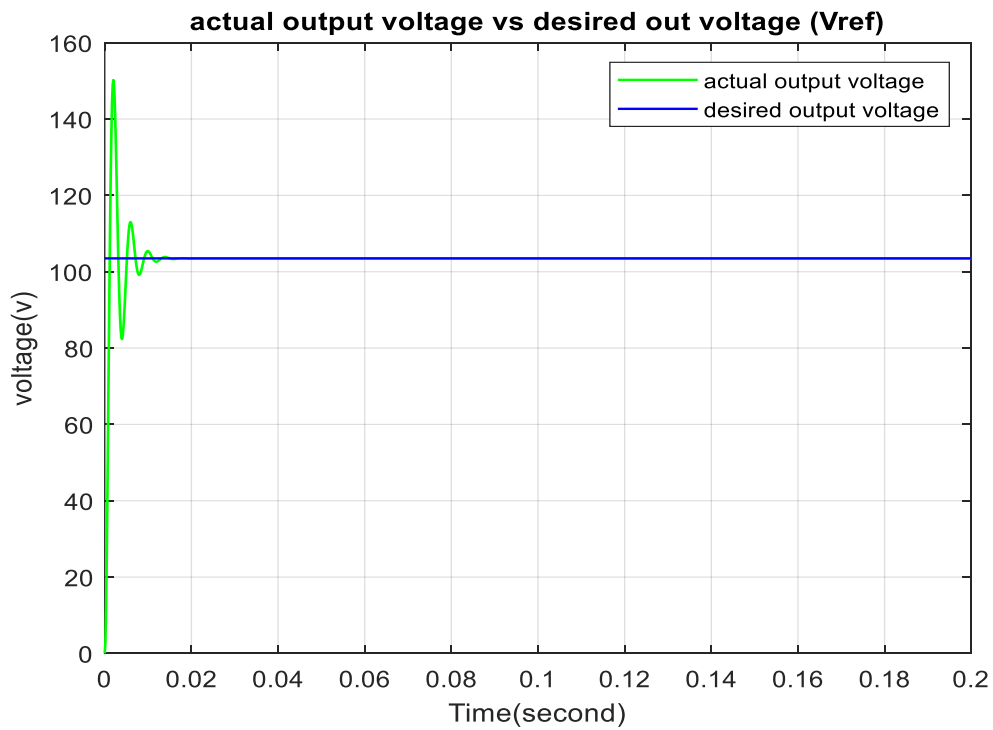


Figure 5.6: Load resistance reduced from 10 into 5

According to the simulation results, The buck converter's output voltage alone exhibits significant overshoot and oscillation. And Also ,when varying the input voltage the convertor output voltage cannot provide the required output voltage (Figure 5.2) and (Figure 5.3) when the input voltage rises, overshoot increases significantly Figure 5.2 .The required output voltage is not affected by reduced load resistance(Figure 5.5).But it increases the overshoot (Figure 5.4). As a result, various controllers are used to solve the problem.

5.3 Buck converter efficiency with a FOPID controller

Figure 5.4 depicts the Simulink block diagram for the system's implemented controller. The fractional controller block is obtained from the FOMCON toolbox. The tuned controller values are used to calculate the performance output index values. The performance of a buck convertor with FOPID and the converter parameters are similar to those in the above (Table 5.1).

A MATLAB/simulink model of a buck regulator using FOPID is shown in Figure 5.4:

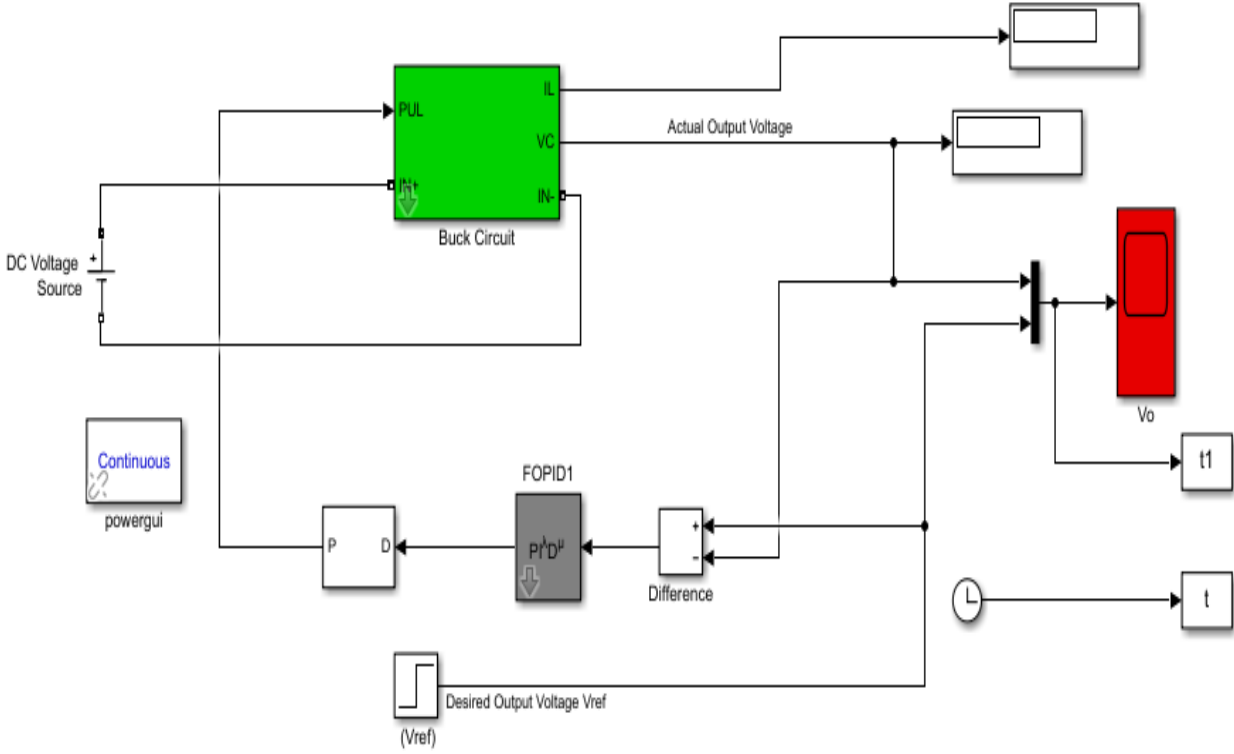


Figure 5.6: Buck converter model in MATLAB/Simulink with FOPID

Table 5.2: FOPID controller parameter

Controller Parameters	FOPID
K_p	74.8553
K_i	94.4285
K_d	91.9714
Δ	0.22307
μ	0.50977

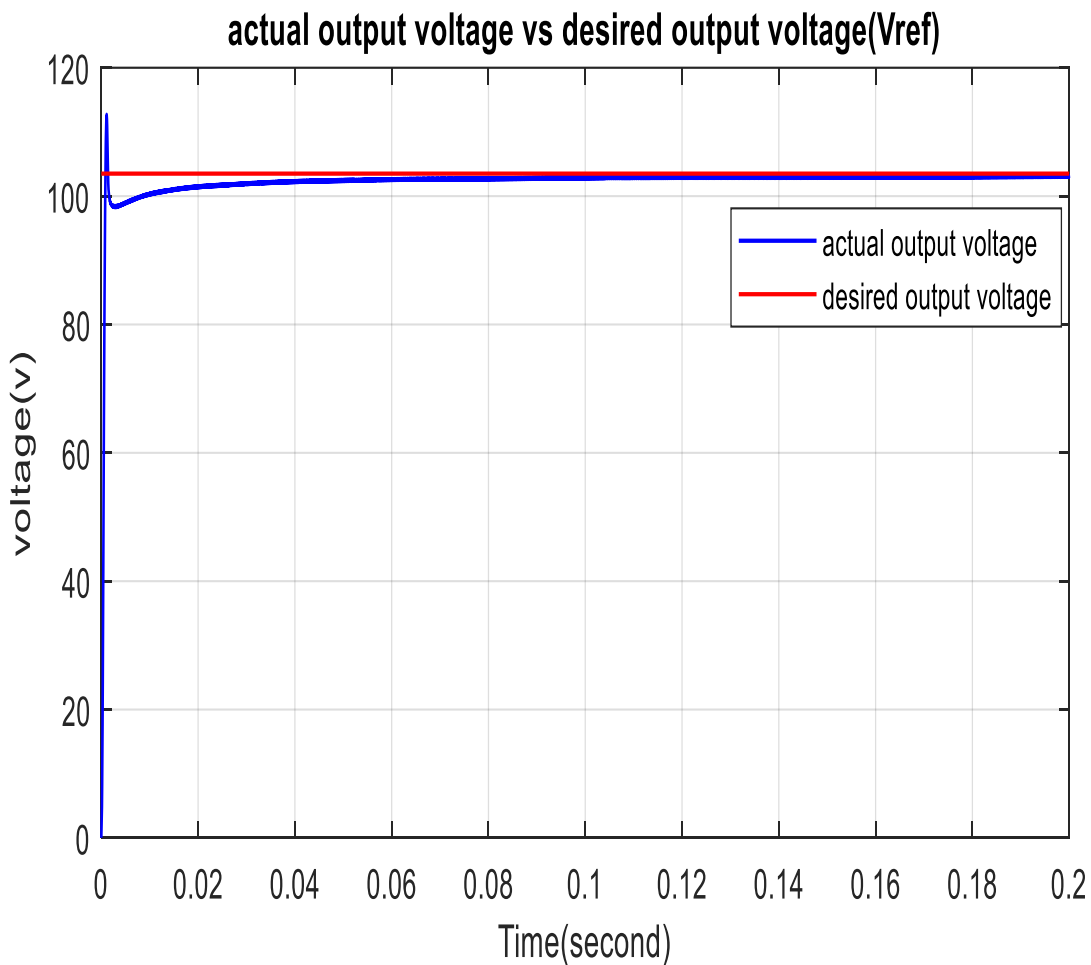
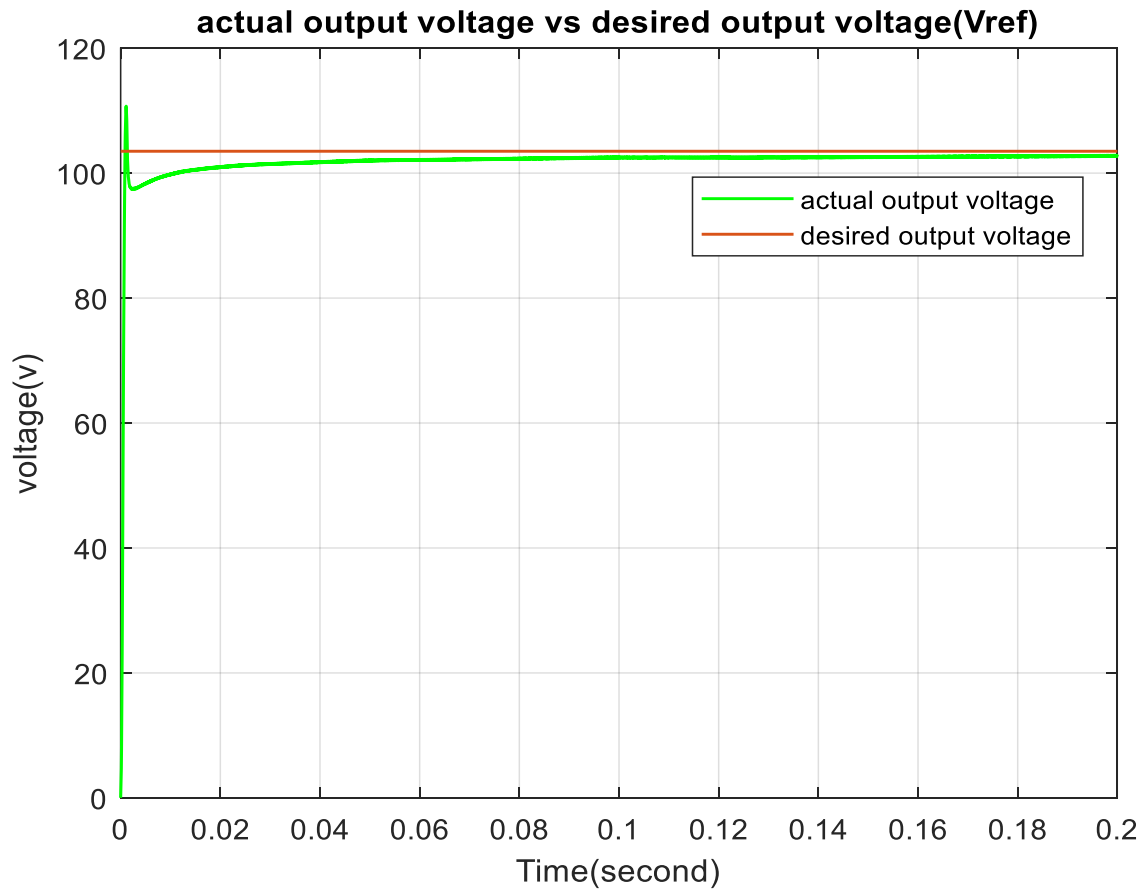


Figure 5.7: Buck converter output voltage using FOPID

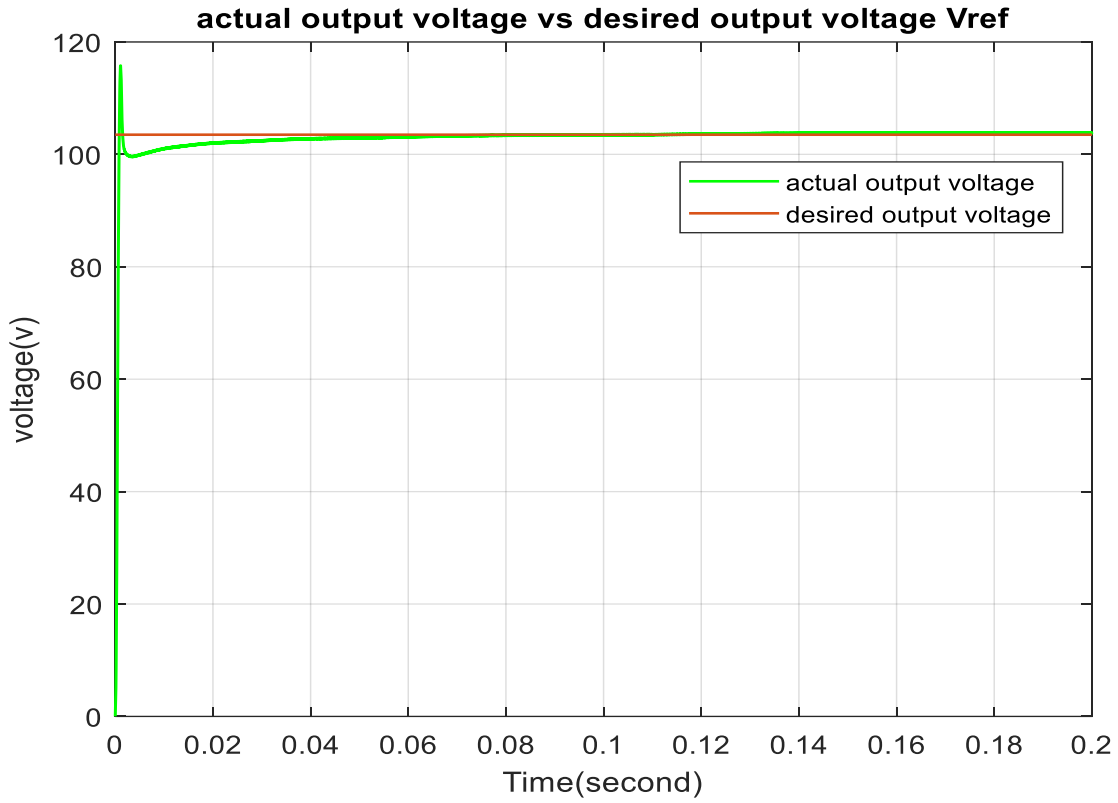
The results shown in figure 5.7, Overshoot is significantly decreased when a buck convertor is used with a FOPID .It dropped from 140.896% to 15.741%. However, as the figure clearly shows, the value of rise and settling time are 0.1600 second and 0.1960 second. The auto tuning of the Fractional Order controller is very computationally intensive

5.4 Buck Converter Performance using FOPID Controller Under Load Resistance and Input Voltage Disturbances

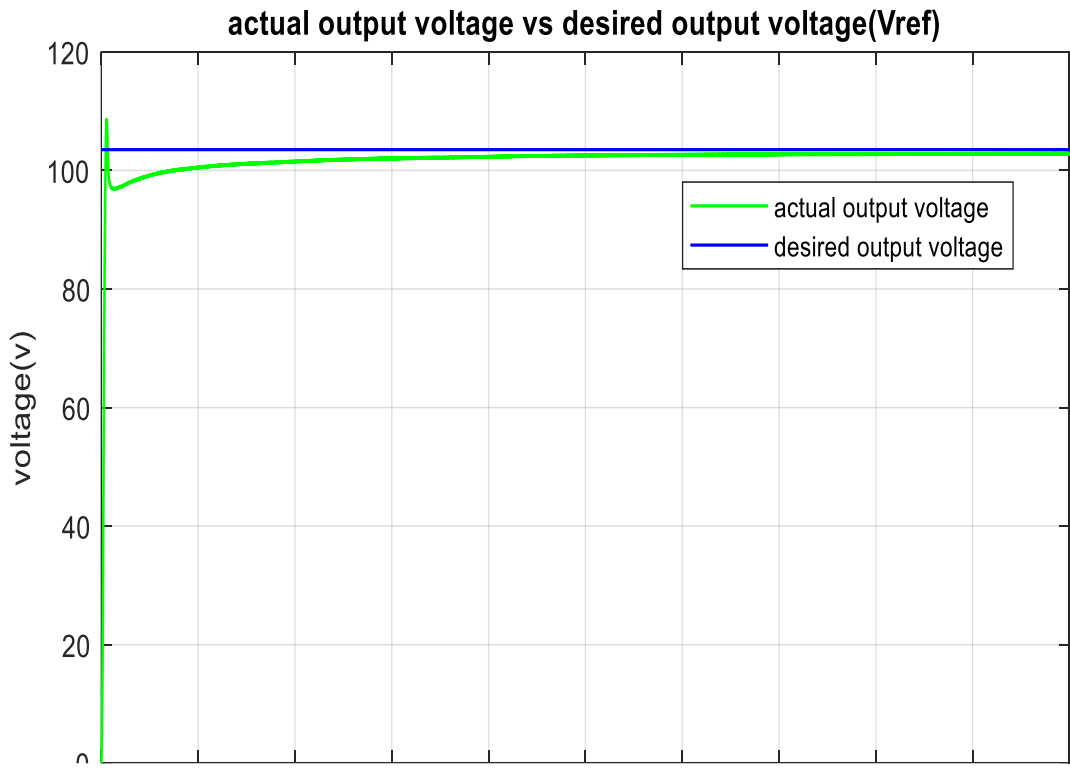
For testing the effectiveness of buck converter increase the input voltage by 13V (220V) & then lowered by 7V (200V). The load resistance is raised from 10 to 13 and then lowered to 5 in order to analyze the effects of load resistance change. Figure 5.6 displays the simulation results.



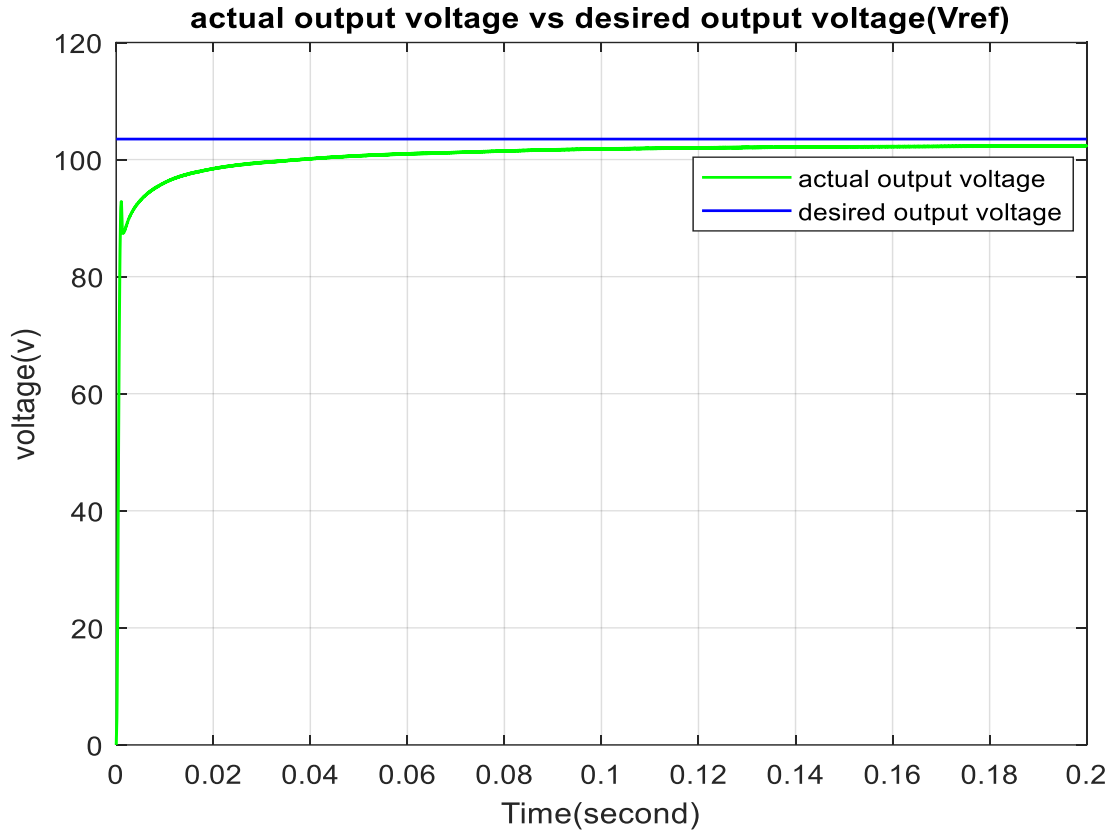
(A)



(B)



(C)



(D)

Figure 5.8: Buck converter simulation results with FOPID by varying load resistance and input voltage.

Figures shown in the above (A) input voltage rise from 207 into 220V; (B) input voltage drop from 207 into 200V; (C) Load resistance raised from 10 into 13; (D) Load resistance reduced from 10 into 5. According to the simulation results shown figure 5.6 the overshoot to a smaller value but settling time and rise time are increased output voltage can be obtained with FOPID. To get the desired output voltage, the converter output voltage is affected by variations in load resistance (Figure 5.8 (C) and (D)).

However, the converter output voltage is unaffected by a reduction the input voltage from the operational point (Figure 5.8 (B)). However, the input voltage is increased from the operational point, the converter provide a continuous desirable output voltage and increase in overshoot, the rise time & settling time are increase (see Figure 5.8 (A)).

This is a result of the nonlinear nature of the buck converter. However, after linearization, the small signal model for the converter was used to develop the linear controllers. This technique's

controllers were unable to act as efficiently to vary in operational point. Due to the converter small signal model changes the operating point. As a result, when the input voltage is increased from the operational point the desirable output voltage is not obtained when using a linear controller. To solve the limitation of linear controllers, nonlinear controllers are important.

5.5 Buck Converter Performance using Super -Twisting Sliding Mode Controller

The converter's parameters are identical to shown in the above table (Table 4.1) To show how well a MATLAB/Simulink DC-DC buck regulators performance with Super Twisting sliding mode controller.

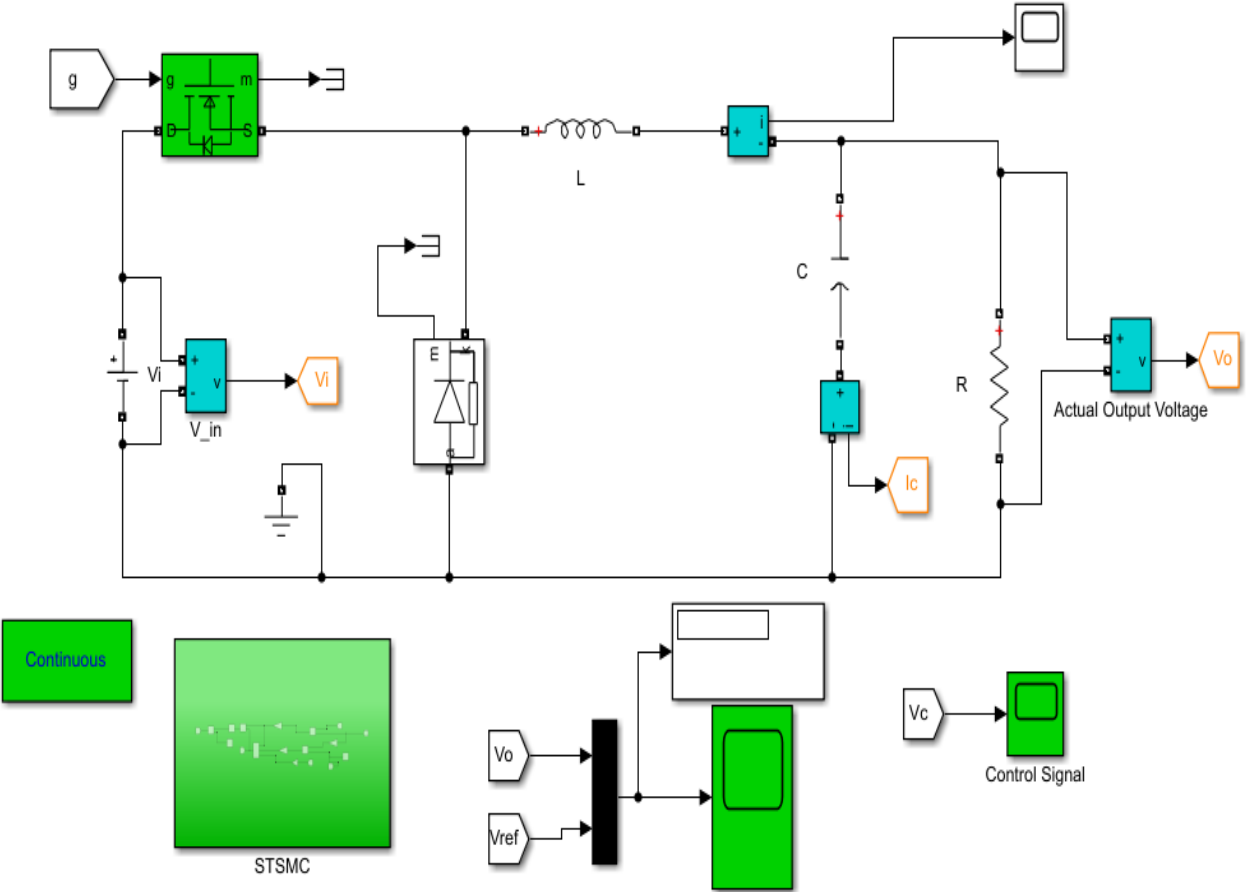


Figure 5.9: Buck converter model in MATLAB/Simulink with Super Twisting sliding mode controller

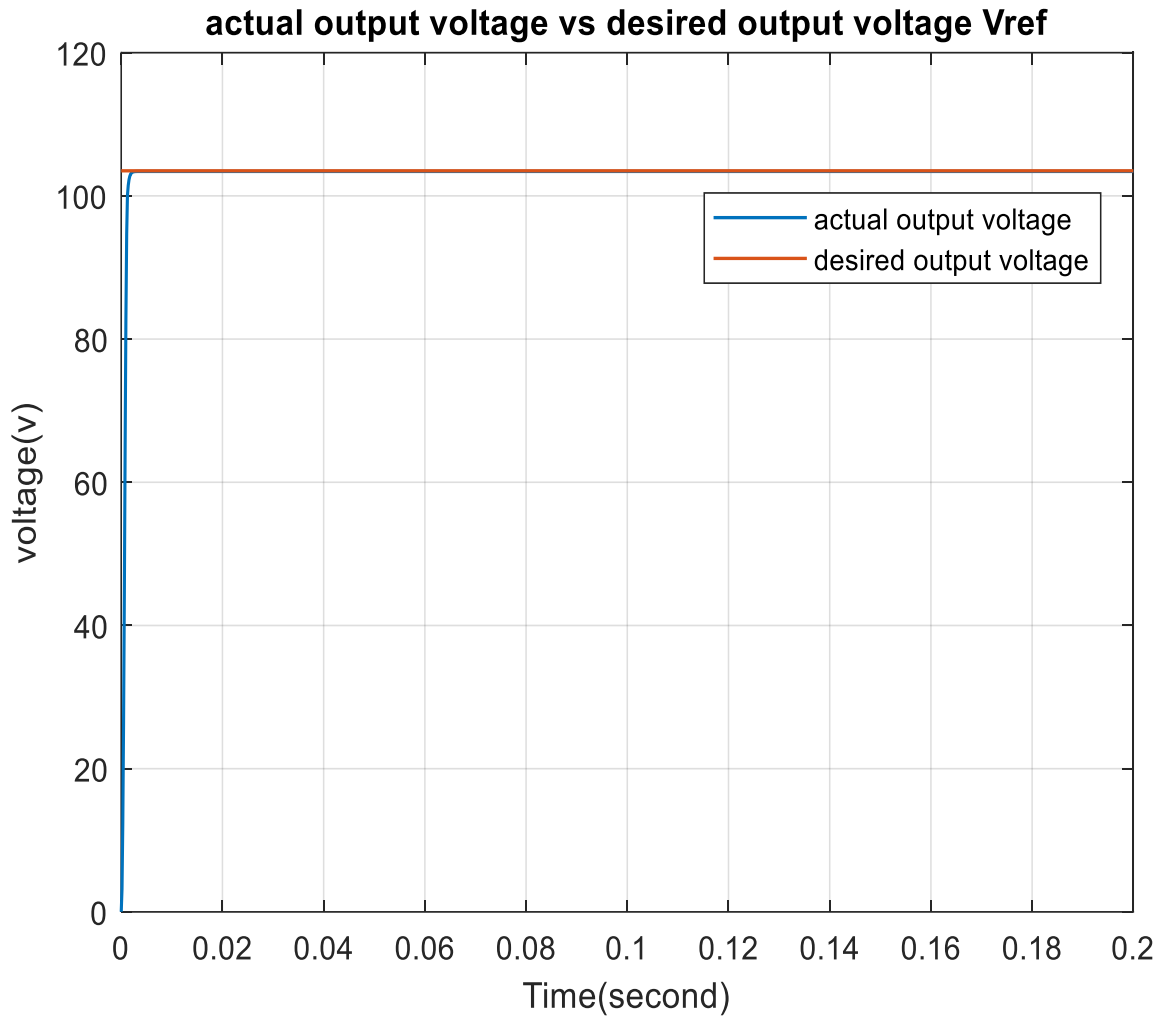
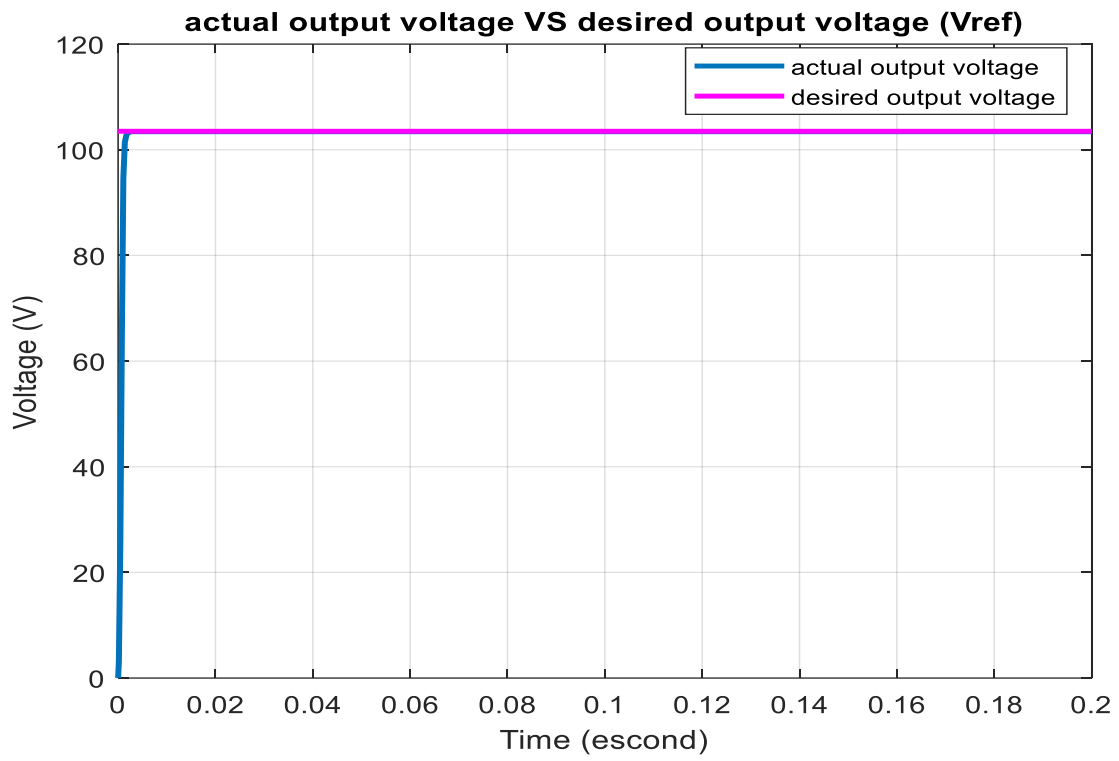


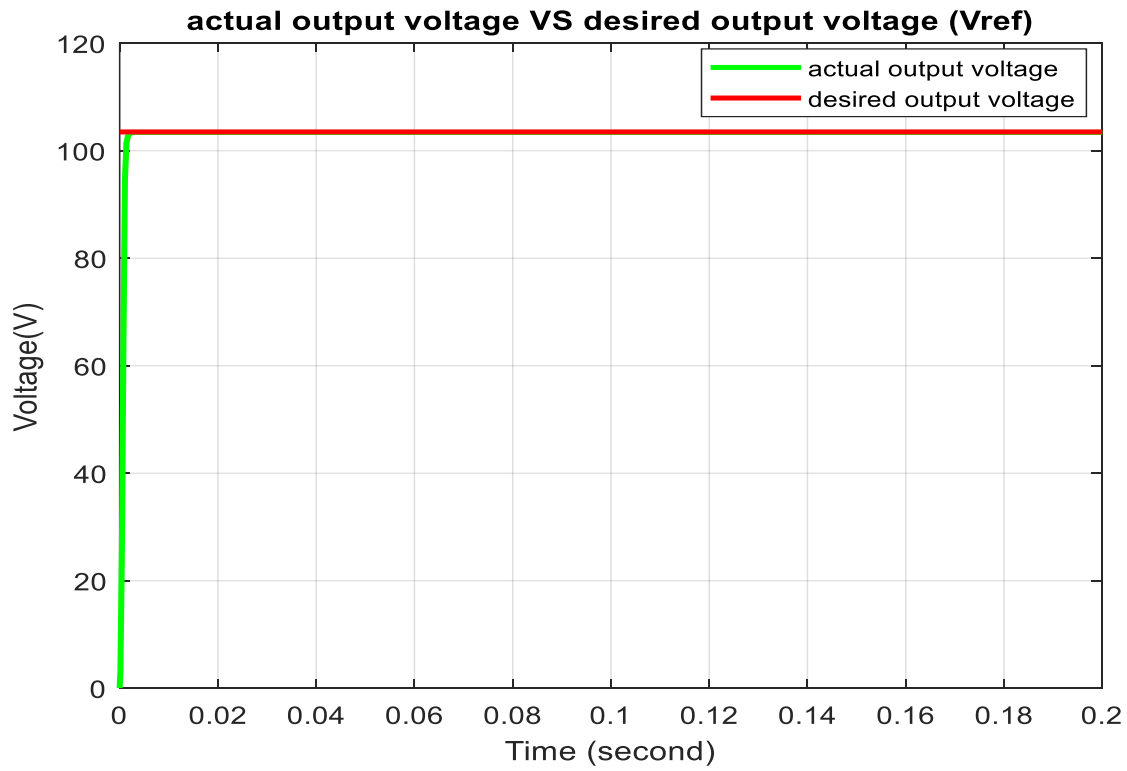
Figure 5.10: the buck converter's output voltage using Super Twisting sliding mode controller. Overshoot is completely eliminated in the result shown in the Figure 5.10 above buck converter utilizing a Super-twisting sliding mode controller. It is possible to get the desirable output voltage with a short rise time and settling times.

5.5 Buck Converter Performance with Super Twisting sliding Mode Controller with Load Resistance and Input Voltage Disturbances

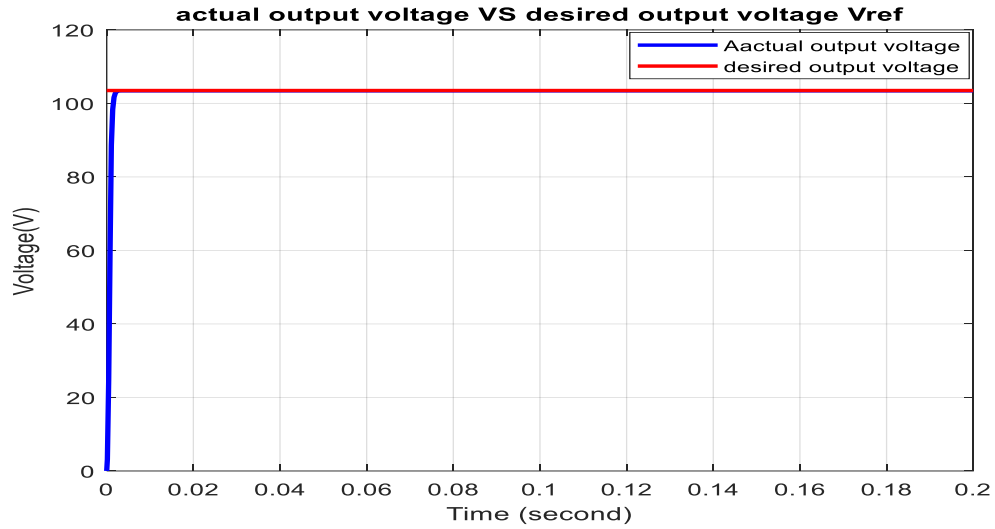
For the purpose of testing the effectiveness of buck converter using super twisting sliding mode controller in input voltage variations, increase the supply voltage by 13V (220) & lowered into 200V. The load resistance was raising from 10 into 13 and then reduced in to 5 to analyse the effect of load resistance change. Figure 5.10 depicts the simulation results



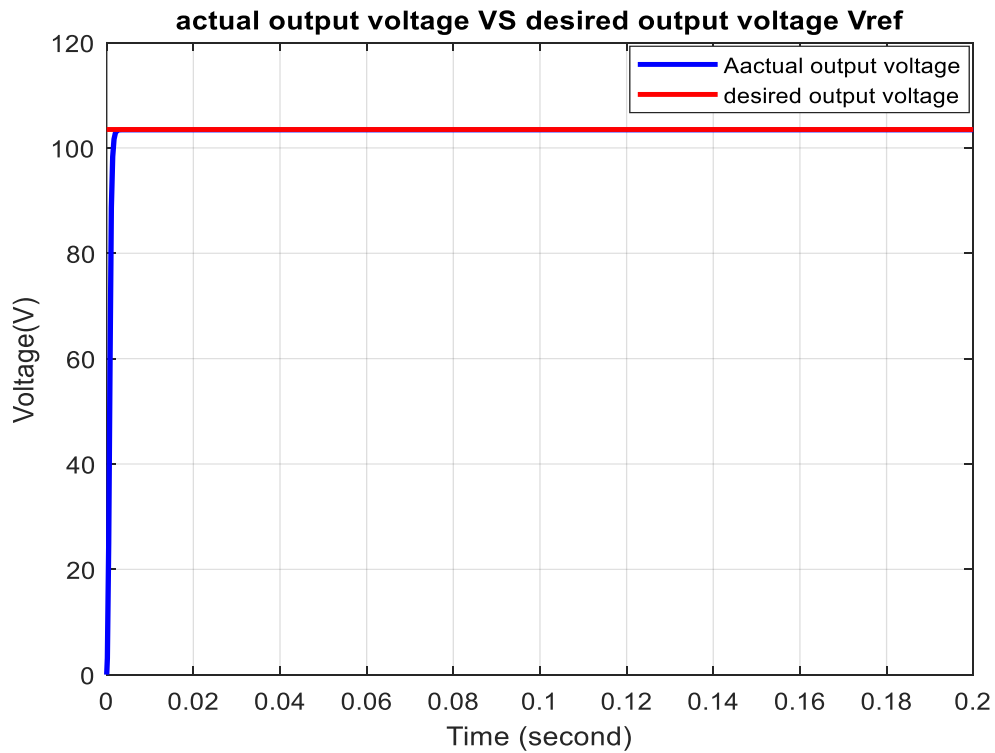
(A)



(B)



(C)



(D)

Figure 5.11: simulation results of a buck convertor using super-twisting sliding mode controller with varying load resistance and input voltage .

(A) input voltage rise from 207 into 220V; (B) input voltage drop from 207 into 200V; (C) Load resistance raised from 10 into 13; (D) Load resistance reduced from 10 into 5.

Based on the results shown in Figure 5.11 For a DC-DC buck convertor, the use of a super-twisting sliding mode controller can compensate for load resistance and input voltage deviations. The desired output voltage and actual output voltage are overlap and if the load resistance and input voltage are varing there is no fluctuation in the desired output voltage.

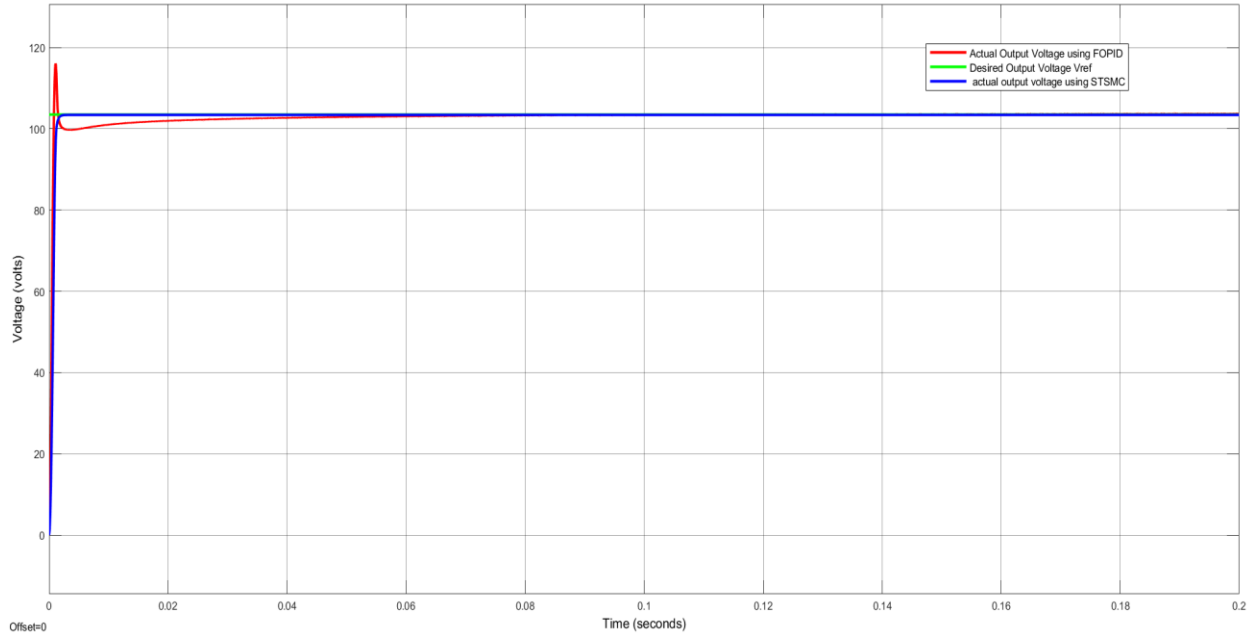
5.7 Performance analysis of FOPID and STSM Controllers

The reference voltage of the buck regulator 103.5V, Figure 5.11 illustrates how STSM control and FOPID response. In terms of settling time and rising time Super-twisting sliding mode controller more fast than FOPID and FOPID has a long rise times and settling times, STSM control has a short rise time and settling time. In the below Figure 5.11 (A) super-twisting sliding mode controller remove the overshoot while the FOPID is decrease from 140.896% into 15.741%. Figure 5.11 (B) shows STSM controller is not affected by input voltage deviation. the input voltage is raising from 207 into 220V the actual output voltage is similar to the desired output voltage. However, using a FOPID controller to raising the input voltage does not produce the desirable output voltage and the input voltage is raising from 207 into 220 V the overshoot is raising by 4.070% beyond the overshoot existence oprational point, from the results of the simulation, it can be stated that the STSM controller performs better than the FOPID controller.

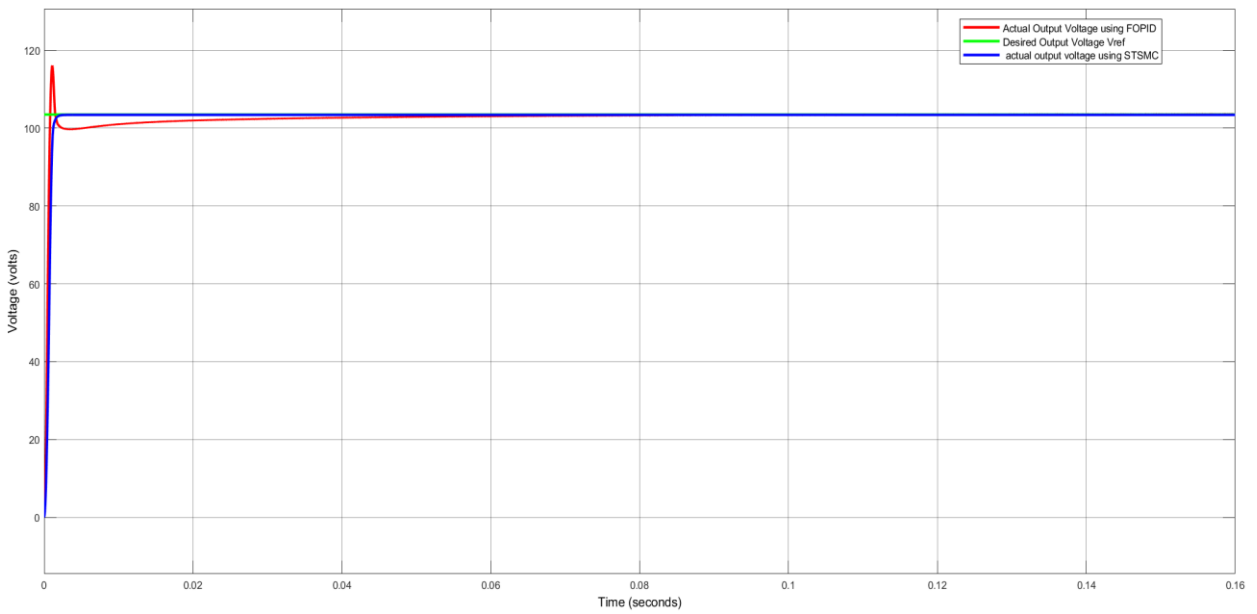
Table 5.3 shows the transient performance and output voltage deviation

Table 5.3: controller performance and output voltage variation.

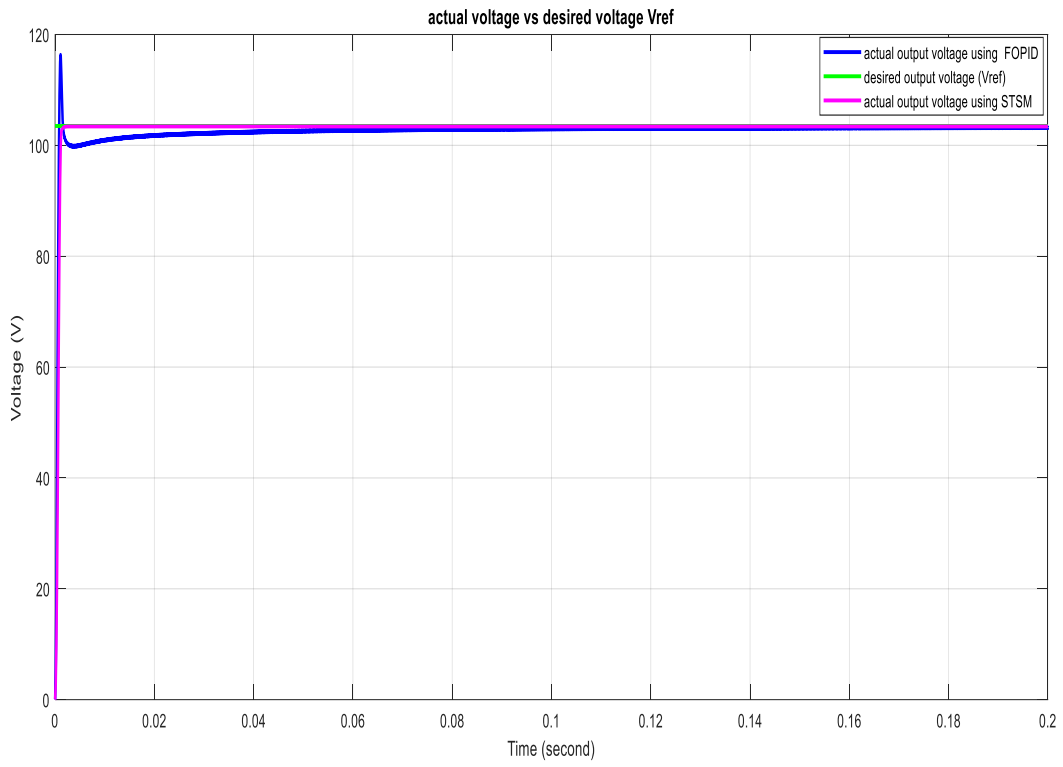
Controller	Output voltage divation for input voltage 207V	Rise time (second)	Settling time (second)	Overshoot (%)
FOPID	---	0.1600	0.1960	15.741
STSM	---	0.0187	0.0229	---



(A)



(B)



(C)

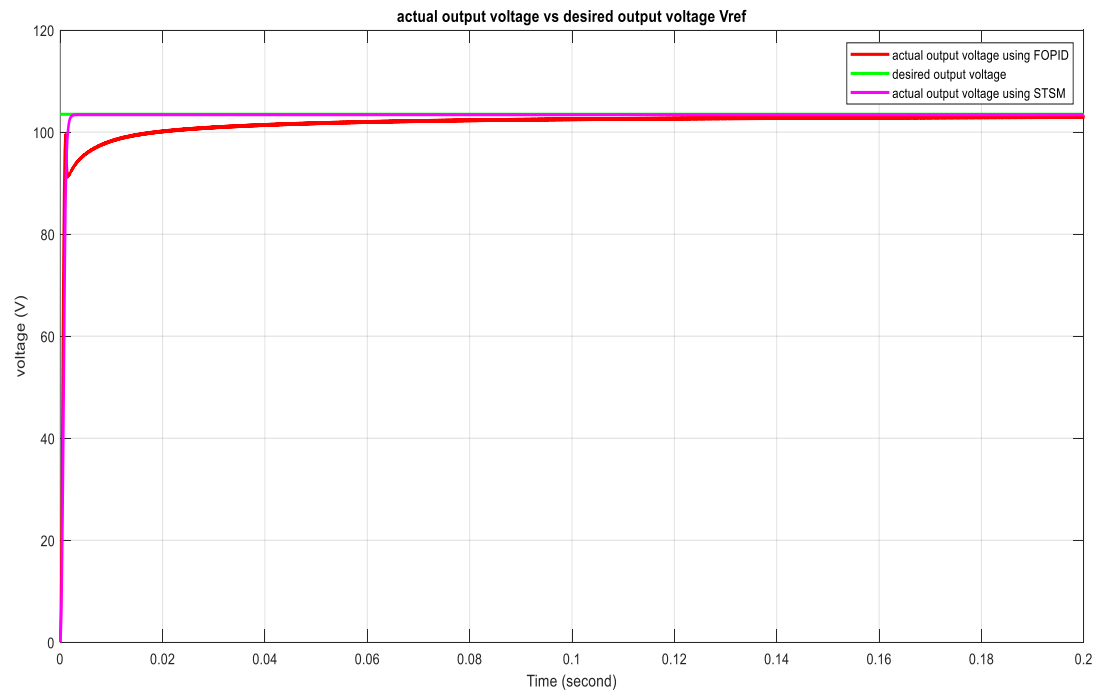


Figure 5.12: Buck converter output voltage with STSMC & FOPID

(A) Buck converter output voltage with STSMC and FOPID control at 207V input . (B) output voltage of a buck convertor when the input voltage is changed from 207V into 220V using STSMC and FOPID control. (C) output voltage of a buck convertor when the resistor is changed from 10ohm into 13 ohm using STSMC and FOPID control. (D) output voltage of a buck convertor when the resistor is changed from 10 ohm into 5 ohm using STSMC and FOPID control.

CHAPTER SIX

CONCLUSION AND FUTURE SCOPE

6.1 CONCLUSION

In this study, two different DC-DC buck converter control strategies are presented. The typical FOPID control is used in the first control approach, while the super-twisting sliding mode (STSM) control method is used in the second, it driven based on super-twisting algorithm. MATLAB/Simulink was used to test the DC-DC buck converter performance of STSMC and FOPID controllers (input voltage and load resistance deviation). When the input voltage is 207V the rise time and settling time is 0.1600second and 0.1960second respectively & the overshoot is decrease from 140.896% into 15.741% using FOPID

However, the settling and rise time in the case of super-twisting sliding mode control is (0.0189 second & 0.0229 second respectively) and there is no overshoot. When the supply voltage is 220V using FOPID the overeshoot is raising from 15.741% into 19.811% , but there is no overshoot using STSMC. Based on the simulation result STSM controller has better performance than FOPID and it has not a chattering . Load resistance varation has an effect on the output voltage using FOPID . But this varation has no effect on the output voltage using STSMC.

6.2 FUTURE SCOPE

Although computer simulations have verified the theory for the voltage regulation of DC-DC buck converters utilizing super-twisting sliding mode control, Investigating its implementation in practice would be good. Testing a different second order sliding mode algorithm besides the currently utilized super twisting approach is another research topic.

REFERENCE

- [1] R. Ildarabadi and A. Ahmadi, "A Review to AC Modeling and Transfer Function of DC-DC Converters," *TELKOMNIKA Indones. J. Electr. Eng.*, vol. 13, no. 2, 2014, doi: 10.11591/telkomnika.v13i2.7033.
- [2] Y. Wang, H. Xia, and Y. Cao, "Voltage Controller of DC-DC Buck Converter Using Terminal Sliding Mode," no. 20122302120012, pp. 262–266, 2015.
- [3] R. L. Gour, "Small Signal Modelling of a Buck Converter using State Space Averaging for Magnet Load," vol. 3, no. 3, pp. 11–17, 2016.
- [4] Y. F. Li, M. F. Tsai, C. S. Tseng, and Y. F. Chiang, "Model reference adaptive control design for the buck-boost converter," *IECON Proc. (Industrial Electron. Conf.)*, pp. 543–548, 2012, doi: 10.1109/IECON.2012.6388768.
- [5] S. V. Adhul and T. Ananthan, "FOPID Controller for Buck Converter," *Procedia Comput. Sci.*, vol. 171, no. 2019, pp. 576–582, 2020, doi: 10.1016/j.procs.2020.04.062.
- [6] A. A. Sahito, M. AslamUqaili, A. SattarLarik, and M. A. Mahar, "Non Linear Controller Design for Buck Converter To Minimize Transient Disturbances.," *Sci. Int.*, vol. 26, no. 3, pp. 1033–1037, 2014, [Online]. Available: <https://search.ebscohost.com/login.aspx?direct=true&db=a9h&AN=99034400&site=ehost-live>.
- [7] V. Behnamgol, A. R. Vali, and I. Mohammadzaman, "Second Order Sliding Mode Control With Finite Time Convergence," 1991, vol. 45, no. 2, pp. 41–52, 2013.
- [8] M. S. Hassan and A. A. Elbaset, "Small-Signal MATLAB/Simulink Model of DC-DC Buck Converter using State-Space Averaging Method," *17 Int. Middle East Power Syst. Conf.*, no. December, pp. S31-66, 2015, doi: 10.13140/RG.2.1.1129.7368.
- [9] M. Algreer, M. Armstrong, and D. Giaouris, "Adaptive PD+I control of a switch-mode DC-DC power converter using a recursive FIR predictor," *IEEE Trans. Ind. Appl.*, vol. 47, no.

- 5, pp. 2135–2144, 2011, doi: 10.1109/TIA.2011.2161856.
- [10] A. Kelly and K. Rinne, “Control of DC-DC converters by direct pole placement and adaptive feedforward gain adjustment,” *Conf. Proc. - IEEE Appl. Power Electron. Conf. Expo. - APEC*, vol. 3, no. May 2014, pp. 1970–1975, 2005, doi: 10.1109/APEC.2005.1453326.
- [11] Y. Huangfu, S. Zhuo, A. K. Rathore, E. Breaz, B. Nahid-Mobarakeh, and F. Gao, “Super-Twisting Differentiator-Based High Order Sliding Mode Voltage Control Design for DC-DC Buck Converters,” *Energies*, vol. 9, no. 7, 2016, doi: 10.3390/en9070494.
- [12] M. Deshmukh, “A Constant Frequency Second Order Sliding Mode Controller for Buck Converter,” *IEEE*, vol. 31, 2017.
- [13] E. R. Lisy, M. Nandakumar, R. Anasraj, and R. K. P, “Design of Robust Chattering free Integral Sliding Mode Controller for Dual Input Buck Boost Converter,” vol. 13, no. 1, pp. 358–365, 2018.
- [14] M. Quamruzzaman and K. M. Rahman, “Fuzzy Logic Based Sliding Mode Controlled DC-DC Boost Converter,” no. December, pp. 18–20, 2010.
- [15] C. Aguilar-Ibanez, J. Moreno-Valenzuela, O. Garcia-Alarcon, M. Martinez-Lopez, J. A. Acosta, and M. S. Suarez-Castanon, “PI-Type Controllers and Σ - Δ Modulation for Saturated DC-DC Buck Power Converters,” *IEEE Access*, vol. 9, pp. 20346–20357, 2021, doi: 10.1109/ACCESS.2021.3054600.
- [16] S. Seshagiri, E. Block, I. Larrea, and L. Soares, “Optimal PID design for voltage mode control of DC-DC buck converters,” *2016 Indian Control Conf. ICC 2016 - Proc.*, no. Icc, pp. 99–104, 2016, doi: 10.1109/INDIANCC.2016.7441112.
- [17] M. Shirazi, R. Zane, and D. Maksimovic, “An autotuning digital controller for DC-DC power converters based on online frequency-response measurement,” *IEEE Trans. Power Electron.*, vol. 24, no. 11, pp. 2578–2588, 2009, doi: 10.1109/TPEL.2009.2029691.
- [18] L. Corradini, P. Mattavelli, W. Stefanutti, and S. Saggini, “Simplified model reference-based autotuning for digitally controlled SMPS,” *IEEE Trans. Power Electron.*, vol. 23, no. 4, pp. 1956–1963, 2008, doi: 10.1109/TPEL.2008.925419.

- [19] H. Sahraoui, S. Drid, L. Chrifi-Alaoui, and M. Hamzaoui, "Voltage control of DC-DC buck converter using second order sliding mode control," 3rd Int. Conf. Control. Eng. Inf. Technol. CEIT 2015, no. May 2015, 2015, doi: 10.1109/CEIT.2015.7233082.
- [20] H. Yigeng and W. Yu, "A robust flyback converter based on high order sliding mode control for fuel cell," IECON Proc. (Industrial Electron. Conf.), pp. 3936–3940, 2014, doi: 10.1109/IECON.2014.7049089.
- [21] K. Riyas and R. Anasraj, "Improved performance of boost converter with super-Twisting algorithm under sliding-mode operation," 2016 Int. Conf. Next Gener. Intell. Syst. ICNGIS 2016, pp. 0–5, 2017, doi: 10.1109/ICNGIS.2016.7854062]]
- [22] Qing-Guo Wang, Zhiping Zhang, Karl Johan Astrom and Lee See Chek, "Guaranteed dominant pole placement with PID controllers," *Journal of Process Control*, vol. 19, pp. 349-352, 2009.
- [23] Jian-Bo He, Qing-Guo Wang, and Tong-Heng Lee, "PI/PID controller tuning via LQR approach," *Chemical Engineering Science*, vol. 55, pp. 2429-2439, 2000. .

Appendix

Appendix A:

The converter is designed for low power application and high switching frequency. So that converter parameters value used for MATLAB/simulink is given as follows:

- The switching frequency is 100 kHz.
- The input voltage is taken as 207V.
- The desired output voltage is 103.5V.
- The load resistance is taken as 10Ω.
- Assume the capacitor ripple voltage is 0.5% of the output voltage.

Based on these parameters it is possible to calculate the minimum inductor that determines the boundary between continuous conduction mode and discontinuous conduction mode and also minimum capacitor to limit ripple voltage below certain value and to minimize overshoot. Using the value given above the duty cycle is given as,

$$D = \frac{V_o}{V_{in}} = \frac{103.5v}{207v} = 0.5$$

The minimum inductor is given as,

$$L_{min} = \frac{(1-D)}{2f} R = \frac{(1-0.5)}{2 * 10^5} * 10 = 25\mu H$$

Since the converter is designed for continuous conduction mode only, the value of inductor should be greater than the minimum value. Therefore to ensure continuous conduction mode of operation the value of inductor is $L=1.5mH$.

The minimum capacitor required is given by,

$$C_{min} = \frac{1 - D}{8\Delta V_o L f^2} V_o = \frac{0.5 * 103.5}{8 * 0.0008625 * 1.5 * 10^{-3} * 10^5} = 51.75\mu f$$

To limit the peak-to-peak value of ripple voltage below a certain value and to minimize the voltage overshoot, the value of capacitor should be greater than the minimum value. For this purpose let the value of capacitor increased by 80% of minimum value of capacitor, so that

$$C_{min} = 250\mu f$$

Appendix B:

$$K_p = \frac{(\omega_n^{cl})^3 + 2m(\xi^{cl})^2(\omega_n^{cl})^4 - (\omega_n^{ol})^2}{K}$$

$$K_p = \frac{(120)^3 + 21(0.148)^2(120)^4 - (1633)^2}{1.3 \times 10^6}$$

$$K_p = 74.8553$$

$$K_i = \frac{m\xi^{cl}(\omega_n^{cl})^4}{K}$$

$$K_i = \frac{4 \times 0.148 \times (120)^4}{1.3 \times 10^6}$$

$$K_i = 94.4285$$

$$K_d = \frac{(2 + m)\xi^{cl}(\omega_n^{cl})^4 - 2\xi^{ol}\omega_n^{ol}}{K}$$

$$K_d = \frac{(2 + 2) \times 0.148 \times (120)^4 - 2 \times 0.123 \times 1633}{1.33 \times 10^6}$$

$$K_d = 92.06$$

Appendix C:

Selecting appropriate value of the L chosen is 1

$$\lambda_1 = \sqrt{L} = \sqrt{1} = 1 \quad \lambda_2 = 2L = 2 \times 1 = 2$$